

We would like to thank the anonymous reviewers and the editor for their careful reading and very important comments. In the following, we replied all the comments point by point.

Anonymous Referee #1

This manuscript combined radiocarbon (^{14}C) and offline-AMS approaches and apportioned sources of organic carbon during an extreme haze episode in China. Here, ^{14}C results were reported for water-soluble OC (WSOC) and water-insoluble OC (WIOC), which enabled a more detailed and straightforward (or accurate) source apportionments of both WSOC and WIOC. Although, radiocarbon measurements of WSOC have been reported in many sites in East Asia and other sites around the world, here the offline-AMS measurements were combined with ^{14}C methods. The fossil and nonfossil sources could be further grouped into primary and secondary sources. Therefore, I think that the method is quite important and may be applied in other regions as well. The results are interesting and informative, which could be applied to some modeling studies in future. The MS could be published in ACP after the author could address the following minor comments.

Reply: We thank the reviewer for the nice summary of our paper and the positive appraisal of the importance of our work. In the following, we replied all the comments point by point.

Comments: In general, how was the relationship between levoglucosan and non-fossil

WSOC (or other OC fractions)?

Reply: We added Figure 4 (see Figure R1 below) in redevised MS. We also added “As shown in Figure 4, non-fossil WSOC was significantly correlated with levoglucosan, indicating that a large fraction of non-fossil WSOC was indeed from biomass burning emissions. In addition, no significant or only a negative correlation (Figure 4) was found between levoglucosan and fraction of fossil to WSOC, suggesting that fossil-fuel source is very unlikely a major or

important contributor of levoglucosan even in the regions (e.g., Xi'an and Beijing in this study) where coal combustion is important.”

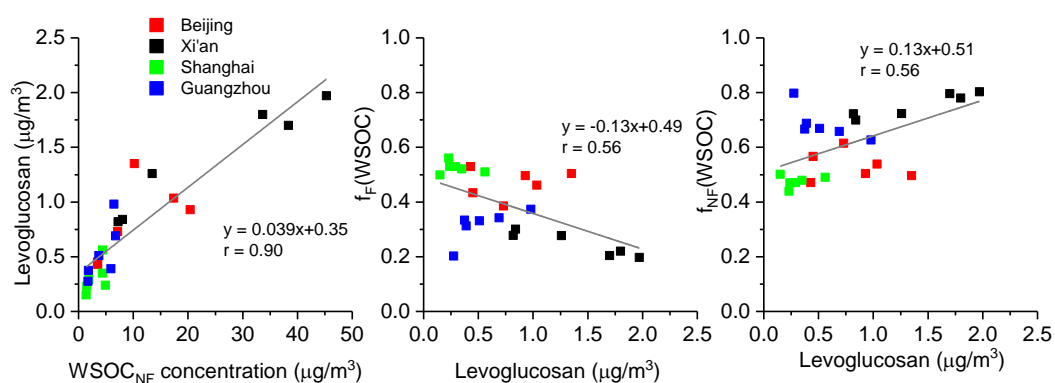


Figure R1. Relationships of non-fossil derived WSOC (WSOC_{NF}) and levoglucosan (left), levoglucosan and fraction of fossil to WSOC ($f_{\text{F}}(\text{WSOC})$) (middle) and levoglucosan and fraction of non-fossil to WSOC ($f_{\text{NF}}(\text{WSOC})$) (right).

In the introduction part, I found the authors seems to miss some important references which have reported most recent source apportionment results in winter haze periods in East Asia.

Reply: The primary objective of this study is to investigate source of WSOC. So we added one more reference about WSOC source apportionment in China (Zong et al., 2016).

“2.3 Offline-AMS measurement and PMF source apportionment” This part is a bit too long, and I suggest the authors only present the most important part and may cite some papers in any using the same method.

Reply: We still think that the detailed information about offline-AMS and PMF is very important, so we would like to keep in the main text. But we revised this part according to the comments from the reviewer 2 (see details below)

Lines 303-304: what were the major sources of non-fossil emissions in Guangzhou and Xi'an?

Reply: The major sources of non-fossil emissions were biomass burning emissions and SOC formation. The detailed WSOC sources were present in the Sec.3.3 (“High contribution of secondary formation to WSOC”) and Figure 7 in revised MS.

Anonymous Referee #2

The manuscript “Large contribution of fossil-fuel derived secondary organic carbon to water-soluble organic aerosols in winter haze of China” deals with the source apportionment of water-soluble organic carbon (WSOC). The sources of this carbon fraction are not well known and few studies exist that focus on the source apportionment of WSOC. Therefore this study is of interest and the combination with aerosol mass spectrometer measurements adds very interesting information of primary vs. secondary organic carbon. Overall, I find the manuscript clearly written and the measurements and calculations thorough and accurate.

In my opinion it can be published after relatively minor revisions.

Reply: We thank the reviewer for the nice summary of our paper and the positive appraisal of the importance of our work. In the following, we replied all the comments point by point.

1) Somewhat major comment: The only point that I don't find very clearly described is section 2.3. This section could maybe be shortened on explaining how the PMF works (e.g. Eq 1 could be omitted), but it should contain more detail on the results of the PMF that are relevant for this work.

1a) Are the PMF results from Huang et al. (2014) directly used, or after some modification? 1b) Explain in more detail how the scaling of the factors works in your case. Eg, in line 135 I do not know what you mean by "here only WSOC PMF is present . . .". I suggest not to mention how Huang et al. (2014) scale their factors, because this is only confusing and not relevant for this work.

Reply: We agree with the reviewer and we have modified the text accordingly. The PMF results from Huang et al. (2014), but only data relative to WSOC are used.

The modifications include the following:

Line 120, we added: Here, only data relative to WSOC are used.

Line 128, we modified the text by removing the explanation about the methodology followed by Huang. The new text reads as follows:

Online AMS measurements provide quantitative mass spectra of submicron non-refractory aerosol species, including organic aerosol and ammonium nitrate and sulfate. However, the offline AMS measurements described herein cannot be directly related to ambient concentrations due to uncertainties in nebulization and AMS lens cut-off. Here, we have scaled the organic aerosol mass spectra to water soluble organic aerosol concentrations

(WSOM), obtained as WSOC times OM/OC ratios. The latter were determined by the high resolution analysis of the organic aerosol mass spectra, acquired by the AMS.

1c) line 158 – 161, give a bit more detail on these factors (preferably in supporting material)

R: We believe that sufficient details were presented in Huang et al. (2014). Here, we will provide only specific details about the identification of these factors. The updated text reads as follows:

Reply: The elements that were constrained in $F_{k,j}$ matrix can be found in Huang et al. (2014). The factors extracted by ME-2 were interpreted to be related to primary emissions from traffic (TR), biomass burning (BB), coal burning (CC), cooking emissions (CI) and dust and from two secondary aerosol fractions. The elements of TR and CI were constrained in the model. BB was identified based on the high contribution of potassium, anhydrous sugars and the fragment $C_2H_4O_2^+$ in the WSOA mass spectrum resulting from the decomposition of the anhydrous sugars. CC, dominant in Beijing, was identified based on the high contribution of PAHs and unsaturated hydrocarbon fragments in the associated WSOA mass spectrum. Dust is identified based on the high contribution of crustal material and calcium. Finally, two secondary mass factors were identified based on the high contribution of secondary inorganic aerosols, including ammonium sulfate and nitrate in their factor profiles and the high oxygenation degree of the associated WSOA.

1c) Eq. 1: you mention s_{ij} , but it is not in the equation?

Reply: S_{ij} , the measurement uncertainty matrix, is not in Eq.1. We were sorry that we made a mistake in the previous main text. The section was revised. PMF uses the uncertainty matrix to scale the residual matrix $E_{i,j}$, and the ratio of quadratic sum of this ratio is minimized iteratively when Equation 1 is solved.

We have updated this section as follows:

PMF solves the bilinear matrix equation:

$$X_{ij} = \sum_k G_{i,k} F_{k,j} + E_{i,j} \quad (\text{Eq. 1})$$

by following a weighted least squares approach. In the equation, i represent the time index, j a species and k the factor number. X_{ij} is the input matrix, $G_{i,k}$ is the matrix of the factor time-series, $F_{k,j}$ is the matrix of the factor profiles and $E_{i,j}$ the model residual matrix. PMF determines $G_{i,k}$ and $F_{k,j}$ such that the ratio of the Frobenius norm of $E_{i,j}$ over the uncertainty matrix, $s_{i,j}$, used as model input is minimised.

1d) line 161 – 162: “The contribution of the water soluble organic aerosol related to these different factors are extracted . . .” How are they extracted?

Reply: The contributions of the water soluble organic aerosol related to these different factors were determined by the multiplying their relative abundance in the factor profiles by the respective factor time-series. The factors WSOM time series were then divided by the respective OM/OC_k calculated from the high-resolution analysis of the factor mass spectral profile to obtain the WSOC_k time series related to each of the factors.

This had been added to the text.

1e) line 162 ff: Please provide more detail: What are “the respective OM/OC_k ratios” for each factor? Please provide values for each factor and more detail on how they were derived. I think the values should be included in the main text, the rest could be in the supporting material.

Reply: The OM/OC_k values were presented in Huang et al., 2014. They were determined from the elemental analysis of the organic fragments in the mass spectra. This is a very

common procedure used by all the AMS community and we do not think that it is necessary to provide more related details. However, we did add the OM/O_{Ck} values in the main text:

The contributions of the water soluble organic aerosol related to these different factors were determined by the multiplying their relative abundance in the factor profiles by the respective factor time-series. The factors WSOM time series were then divided by the respective OM/O_{Ck} calculated from the high-resolution analysis of the factor mass spectral profile to obtain the WSOC_k time series related to each of the factors. The average OM/O_{Ck} are: 1.25, 1.39, 1.49, 1.55, 2.25, and 2.4 for TR, CI, BB, CB, SOA, and dust, respectively.

Minor comments: 2) Line 191ff: Please give a bit more detail on how you estimate the factor 1.08.

Reply: The detailed calculation is explained in (Zhang et al., 2012). The reference is added now. See “ $f_{\text{NF}}(\text{ref})$ is a reference value representing f_{M} of non-fossil sources during the sampling periods, which can be further separated into biogenic (bio) and biomass-burning (bb) sources given that other non-fossil sources (e.g. cooking and biofuel combustion) are negligible. Hence, $f_{\text{NF}}(\text{ref})$ is defined as:

$$f_{\text{NF}}(\text{ref}) = p_{\text{bio}} \times f_{\text{bio}}(\text{ref}) + (1 - p_{\text{bio}}) \times f_{\text{bb}}(\text{ref})$$

where p_{bio} refers to the percent of the biogenic sources to the total non-fossil sources; $f_{\text{bb}}(\text{ref})$ can be retrieved from a tree-growth model according to (Mohn et al., 2008), and $f_{\text{bio}}(\text{ref})$ from the long-term time series of ¹⁴CO₂ measurements in atmosphere at the Schauinsland station (Levin et al., 2010). In the case of source apportionment of OC, p_{bio} can be simply estimated as a constant value (e.g. 50%) given that the variations of $f_{\text{NF}}(\text{ref})$ produced by different p_{bio} values are relatively small, especially if compared to the measurement and method uncertainties (Minguillón et al., 2011). And in the case of EC, p_{bio} is zero as biomass burning is the only source of non-fossil EC.” Here, $f_{\text{NF}}(\text{ref})=0.5*1.1+0.5*1.05$, approaching 1.08. We

changed the sentence as “ $f_{M,ref}$ is a reference value of f_M for non-fossil carbon sources including biogenic and biomass burning emissions, which were estimated as 1.08 ± 0.05 (i.e., $f_{M,ref} = (0.5 * 1.10 + 0.5 * 1.05)$ (see details in (Zhang et al., 2012)) for WSOC samples collected in 2013 according to the contemporary atmospheric CO_2 f_M (Levin et al., 2010) and a tree growth model (Mohn et al., 2008).”.

3) Line 236-254: You start the result section with a summary of previous findings of other papers. This would fit better in the introduction

Reply: this section is aiming to make comparisons between our study and other studies to show a board implication, so we would like to keep the discussion here.

4) line 252: “(three with the highest three with average PM mass)” At first I was confused by this, but I believe that there is just a comma missing?

Reply: A comma was added.

5) Table 1: Since you have relatively few data points from PM2.5 samples in Europe, I suggest to take a look at a recent publication that also had data related to fossil and non-fossil WSOC. Maybe some useful information can be found in that. Dusek, U., et al., Sources and formation mechanisms of carbonaceous aerosol at a regional background site in the Netherlands: Insights from a year-long radiocarbon study, Atmos. Chem. Phys., 17, 1-19, 2017.

Reply: Thanks! We added it.

6) Please correct minor grammatical errors throughout the manuscript ... e.g. the example from above: "The contribution of the water soluble organic aerosol related to these different factors are extracted . . .", should either read "The contribution ... IS extracted" or "the contributionS ... are extracted" I noticed several similar instances throughout the manuscript.

Reply: Yes. We checked grammatical errors throughout the manuscript

References

Levin, I., Naegler, T., Kromer, B., Diehl, M., Francey, R. J., Gomez-Pelaez, A. J., Steele, L. P., Wagenbach, D., Weller, R., and Worthy, D. E.: Observations and modelling of the global distribution and long-term trend of atmospheric $^{14}\text{CO}_2$, *Tellus B*, 62, 26-46, 2010.

Mohn, J., Szidat, S., Fellner, J., Rechberger, H., Quartier, R., Buchmann, B., and Emmenegger, L.: Determination of biogenic and fossil CO_2 emitted by waste incineration based on $^{14}\text{CO}_2$ and mass balances, *Bioresour. Technol.*, 99, 6471-6479, 2008.

Zhang, Y. L., Perron, N., Ciobanu, V. G., Zotter, P., Minguillón, M. C., Wacker, L., Prévôt, A. S. H., Baltensperger, U., and Szidat, S.: On the isolation of OC and EC and the optimal strategy of radiocarbon-based source apportionment of carbonaceous aerosols, *Atmos. Chem. Phys.*, 12, 10841-10856, 2012.

Zong, Z., Wang, X., Tian, C., Chen, Y., Han, G., Li, J., and Zhang, G.: Source and formation characteristics of water-soluble organic carbon in the anthropogenic-influenced Yellow River Delta, North China, *Atmos. Environ.*, 144, 124-132, 2016.

1 author's changes in manuscript (highlight)

2 **Large contribution of fossil-fuel derived secondary organic**
3 **carbon to water-soluble organic aerosols in winter haze of China**

4 Yan-Lin Zhang^{1,2,3*}, Imad El-Haddad³, Ru-Jin Huang^{3,4*}, Kin-Fai Ho^{4,5}, Jun-Ji Cao^{4*},
5 Yongming Han⁴, Peter Zotter^{3,#}, Carlo Bozzetti³, Kaspar R. Daellenbach³, Jay G. Slowik³, Gary
6 Salazar², André S.H. Prévôt^{3*}, Sönke Szidat^{2*}

7 ¹Yale-NUIST Center on Atmospheric Environment, Nanjing University of Information Science
8 and Technology, 210044 Nanjing, China

9 ²Department of Chemistry and Biochemistry & Oeschger Centre for Climate Change Research,
10 University of Bern, 3012 Bern, Switzerland

11 ³Paul Scherrer Institute (PSI), 5232 Villigen, Switzerland

12 ⁴Key Laboratory of Aerosol Chemistry and Physics, Institute of Earth Environment, Chinese
13 Academy of Sciences, 710061 Xi'an, China

14 ⁵School of Public Health and Primary Care, The Chinese University of Hong Kong, Hong Kong,
15 China

16 *To whom correspondence should be addressed. E-mail: dryanlinzhang@outlook.com or
17 zhangyanlin@nuist.edu.cn (Y.-L.Z.); andre.prevot@psi.ch (A. Prévôt); rujin.huang@ieecas.cn
18 (R.-J.H.); jjcao@ieecas.cn (J.J.C.); szidat@dcb.unibe.ch (S.S.).

19 Phone: +86 25 5873 1022; fax: +86 25 5873 1193

20 **Abstract**

21 Water-soluble organic carbon (WSOC) is a large fraction of organic aerosols (OA) globally and
22 has significant impacts on climate and human health. The sources of WSOC remain very
23 uncertain in polluted regions. Here we present a quantitative source apportionment of WSOC
24 isolated from aerosols in China using radiocarbon (^{14}C) and offline high-resolution time-of-
25 flight aerosol mass spectrometer measurements. Fossil emissions on average accounted for 32-
26 47% of WSOC. Secondary organic carbon (SOC) dominated both the non-fossil and fossil
27 derived WSOC, highlighting the importance of secondary formation to WSOC in severe winter
28 haze episodes. Contributions from fossil emissions to SOC were $61\pm 4\%$ and $50\pm 9\%$ in
29 Shanghai and Beijing, respectively, significantly larger than those in Guangzhou ($36\pm 9\%$) and
30 Xi'an ($26\pm 9\%$). The most important primary sources were biomass burning emissions,
31 contributing 17-26% of WSOC. The remaining primary sources such as coal combustion,
32 cooking and traffic were generally very small but not negligible contributors, as coal
33 combustion contribution could exceed 10%. Taken together with earlier ^{14}C source
34 apportionment studies in urban, rural, semi-urban, and background regions in Asia, Europe and
35 USA, we demonstrated a dominant contribution of non-fossil emissions (i.e., $75\pm 11\%$) to
36 WSOC aerosols in the North Hemisphere; however, the fossil fraction is substantially larger in
37 aerosols from East Asia and the East Asian pollution outflow especially during winter due to
38 increasing coal combustion. Inclusion of our findings can improve a modelling of effects of
39 WSOC aerosols on climate, atmospheric chemistry and public health.

40 **1 INTRODUCTION**

41 Water-soluble organic carbon (WSOC) is a large fraction of atmospheric organic
42 aerosols (OA), which contributes approximately 10% to 80% of the total mass of organic carbon
43 (OC) in aerosols from urban, rural and remote sites (Zappoli et al., 1999;Weber et al.,
44 2007;Ruellan and Cachier, 2001;Wozniak et al., 2012;Mayol-Bracero et al., 2002). Only 10 to
45 20% of total mass of WSOC has been resolved at a molecular level, and it consists of a large
46 variety of chemical species such as mono- and di-carboxylic acids, carbohydrate derivatives,
47 alcohols, aliphatic and aromatic acids and amino acids (Fu et al., 2015;Noziere et al., 2015).
48 Recent studies suggest that the water-soluble fraction of HUmic LIke Substances (HULIS) is
49 a major component of WSOC, which exhibits light-absorbing properties (Limbeck et al.,
50 2005;Andreae and Gelencser, 2006;Laskin et al., 2015). Therefore, WSOC has significant
51 influences on the Earth's climate either directly by scattering and absorbing radiation or
52 indirectly by altering the hygroscopic properties of aerosols and increasing cloud condensation
53 nuclei (CCN) activity (Asa-Awuku et al., 2011;Cheng et al., 2011;Hecobian et al., 2010).

54 WSOC can be directly emitted as primary particles mainly from biomass burning
55 emissions or produced from secondary organic aerosol (SOA) formation (Sannigrahi et al.,
56 2006;Kondo et al., 2007;Weber et al., 2007;Bozzetti et al., 2017b;Bozzetti et al., 2017a).
57 Ambient studies provide evidence that SOA formation through the oxidation of volatile organic
58 compounds (VOCs) and gas-to-particle conversion processes may be a prevalent source of
59 WSOC (Kondo et al., 2007;Weber et al., 2007;Miyazaki et al., 2006;Hecobian et al., 2010).
60 WSOC is therefore thought to be a good proxy of secondary organic carbon (SOC) in the
61 absence of biomass burning (Weber et al., 2007). By contrast, water-insoluble OC (WIOC) is
62 thought to be mainly from primary origins with a substantial contribution from fossil fuel
63 emissions (Miyazaki et al., 2006;Zhang et al., 2014b).

64 Due to a large variety of sources and unresolved formation processes of WSOC, their
65 relative fossil and non-fossil contributions are still poorly constrained. Radiocarbon (^{14}C)
66 analysis of sub-fractions of organic aerosols such as OC, WIOC and WSOC enable an

67 unambiguous, precise and quantitative determination of their fossil and non-fossil sources
68 (Zhang et al., 2012;Zhang et al., 2014b;Zhang et al., 2014c;Zong et al., 2016;Cao et al., 2017).
69 Meanwhile, the application of aerosol mass spectrometer measurement and positive matrix
70 factorization and multi-linear engine 2 (ME-2) can quantitatively classify organic aerosols into
71 two major types such as hydrocarbon-like OA (HOA) from primary fossil-fuel combustion and
72 oxygenated organic aerosol (OOA) from secondary origin (Zhang et al., 2007;Jimenez et al.,
73 2009). Field campaigns with the aerosol mass spectrometer (AMS) have revealed a
74 predominance of OOA in various atmospheric environments, although their sources remain
75 poorly characterized (Zhang et al., 2007;Jimenez et al., 2009). Previous studies found OOA is
76 strongly correlated with WSOC from urban aerosols in Tokyo, Japan, the Pearl River Delta
77 (PRD) in South China and Helsinki, Finland, indicating similar chemical characteristics,
78 sources and formation processes of OOA and WSOC (Kondo et al., 2007;Xiao et al.,
79 2011;Timonen et al., 2013). Similarly, HOA is mostly water insoluble and the major portion of
80 water insoluble OC (WIOC) can be assigned as HOA (Kondo et al., 2007;Daellenbach et al.,
81 2016). Therefore, ^{14}C measurement of WIOC and WSOC aerosols may provide new insights
82 into sources and formation processes of primary and secondary OA, respectively, which also
83 will elucidate the origin of HOA and OOA as measured by AMS (Zotter et al., 2014b;Zhang et
84 al., 2017).

85 In this paper we apply a newly developed method to measure ^{14}C in WSOC of $\text{PM}_{2.5}$
86 (particulate matter with an aerodynamic diameter of small than $2.5\ \mu\text{m}$) samples collected at
87 four Chinese megacities during an extremely severe haze episode during winter 2013 (Zhang
88 et al., 2015b;Huang et al., 2014). In conjunction with our previous dataset from the same
89 campaign, we quantify fossil and non-fossil emissions from primary and secondary sources of
90 WSOC and WIOC. The dataset is also complemented by previous ^{14}C -based source
91 apportionment studies conducted in urban, rural and remote regions in the North Hemisphere
92 to gain an overall picture of the sources of WSOC aerosols.

93 **2 MATERIALS AND METHODS**

94 **2.1 Sampling**

95 During January 2013 extremely high concentrations of 24-h PM_{2.5} (i.e. often >100
96 µg/m³) were identified in several large cities in East China (Huang et al., 2014;Zhang et al.,
97 2015b). To investigate sources and formation mechanisms of the haze particles, an intensive
98 field campaign was carried out in four large cities, Beijing, Xi'an, Shanghai and Guangzhou,
99 which are representative cities of the Beijing-Tianjin-Hebei region, central-northwest region,
100 Yangtze Delta Region, and Pearl River Delta Region, respectively. The sampling procedures
101 have been previously described in detail elsewhere (Zhang et al., 2015b). Briefly, PM_{2.5} samples
102 were collected on pre-baked (450 °C for 6 hours) quartz filters using high-volume samplers for
103 24 h at a flow rate of ~1.05 m³/min from 5 to 25 January 2013. The sampling sites in each city
104 were located at campuses of universities or at research institutes, at least 100 m away from
105 major emission sources (e.g., roadways, industry and domestic sources). One field blank sample
106 for each site was collected and analyzed. The results reported here were corrected for these field
107 blanks (Zotter et al., 2014a;Cao et al., 2013). All samples were stored at -20 °C before analysis.
108 The PM_{2.5} mass was gravimetrically measured with an analytical microbalance before and after
109 sampling with the same conditions (~12 hour)

110 **2.2 OC and EC mass determinations**

111 A 1.0 cm² filter punches were used for OC and EC mass determination with a OC/EC
112 analyzer (Model4L) using the EUSAAR_2 protocol (Cavalli et al., 2010). The replicate analysis
113 (n=6) showed an analytical precision with relative standard deviations smaller than 5%, 10%,
114 and 5% for OC, EC and TC, respectively. The field blank of OC was on average 2.0 ± 1.0
115 µg/cm² (equivalent to ~0.5 µg/m³), which was used for blank correction for OC. EC data was
116 not corrected for field blank, because such a blank was not detectable.

117 **2.3 Offline-AMS measurement and PMF source apportionment**

118 The water-soluble extracts from the same samples were analyzed by a high-resolution time of
119 flight aerosol mass spectrometer (HR-ToF-AMS) and the resulting mass spectra were used as

120 an inputs for positive matrix factorization (PMF) for the source apportionment of the WSOC,
121 OC and PM_{2.5}. The methodology applied, and the AMS-PMF results obtained are detailed in
122 Huang et al. (2014) and will only be briefly described in the following. Here, only data relative
123 to WSOC are used.

124 Filter punches (the equivalent of ~4 cm²) were sonicated in 10 mL ultrapure water (18.2 MΩ
125 cm at 25 °C, TOC <3ppb) for 20 min at 30°C. The water extracts were aerosolized and the
126 resulting particles were dried with a silica gel diffusion dryer before analysis by the HR-ToF-
127 AMS. For each measurement ten mass spectra were recorded (AMS V-mode, m/z 12-500), with
128 a collection time for each spectrum of 1 minute.

129 Online AMS measurements provide quantitative mass spectra of submicron non-refractory
130 aerosol species, including organic aerosol and ammonium nitrate and sulfate. However, the
131 offline AMS measurements described herein cannot be directly related to ambient
132 concentrations due to uncertainties in nebulization and AMS lens cut-off. Here, we have
133 scaled the organic aerosol mass spectra to water soluble organic aerosol concentrations
134 (WSOM), obtained as WSOC times OM/OC ratios. The latter were determined by the high
135 resolution analysis of the organic aerosol mass spectra, acquired by the AMS.

136 The quantitative WSOM mass spectra are used together with other aerosol species (listed
137 below), collectively referred to as ‘species’ hereafter, as PMF inputs. PMF solves the bilinear
138 matrix equation:

$$139 \quad X_{ij} = \sum_k G_{i,k} F_{k,j} + E_{i,j} \quad (\text{Eq. 1})$$

140 by following a weighted least squares approach. In the equation, i represent the time index, j a
141 species and k the factor number. X_{ij} is the input matrix, $G_{i,k}$ is the matrix of the factor time-
142 series, $F_{k,j}$ is the matrix of the factor profiles and $E_{i,j}$ the model residual matrix. PMF
143 determines $G_{i,k}$ and $F_{k,j}$ such that the ratio of the Frobenius norm of $E_{i,j}$ over the uncertainty
144 matrix, $s_{i,j}$, used as model input is minimised.

145 The species considered as inputs include the quantitative WSOM mass spectra, organic markers
146 (3 anhydrous sugars, 4 lignin breakdown products, 2 resin acids, 4 hopanes, 19 polycyclic
147 aromatic hydrocarbons and their oxygenated derivatives), EC, and major ions (Cl^- , NO_3^- , SO_4^{2-} ,
148 oxalate, methylsulfonic acid, Na^+ , K^+ , Mg^{2+} , Ca^{2+} , and NH_4^+) and residual PM. The latter is the
149 difference between total $\text{PM}_{2.5}$ mass and the measured species. It represents our best estimate
150 of the particulate chemical species not measured here, most likely dominated by crustal material.

151 The Source Finder toolkit (SoFi v.4.9) (Canonaco et al., 2013) for IGOR Pro software package
152 (Wavemetrics, Inc., Portland, OR, USA) was used to run the PMF algorithm. The PMF was
153 solved by the Multilinear Engine 2 (ME-2, Paatero, 1999), which allows the constraining of the
154 $F_{k,j}$ elements to vary within a certain range defined by the scalar α ($0 \leq \alpha \leq 1$), such that the
155 modelled $F'_{k,j}$ equals:

$$156 \quad F'_{k,j} = F_{k,j} \pm \alpha * F_{k,j} \quad (\text{Eq. 2})$$

157 The elements that were constrained in $F_{k,j}$ matrix can be found in Huang et al. (2014). The
158 factors extracted by ME-2 were interpreted to be related to primary emissions from traffic (TR),
159 biomass burning (BB), coal burning (CC), cooking emissions (CI) and dust and from two
160 secondary aerosol fractions. The contributions of the water soluble organic aerosol related to
161 these different factors were determined by the multiplying their relative abundance in the factor
162 profiles by the respective factor time-series. The factors WSOM time series were then divided
163 by the respective OM/OC_k calculated from the high-resolution analysis of the factor mass
164 spectral profile to obtain the WSOC_k time series related to each of the factors. The average
165 OM/OC_k are: 1.25, 1.39, 1.49, 1.55, 2.25, and 2.4 for TR, CI, BB, CB, SOA, and dust,
166 respectively. In the following analysis, the mass of WSOC_k related to coal burning and traffic
167 were assigned to fossil WSOC fraction, while the mass of WSOC_k related to biomass burning
168 and cooking emissions were assigned to non-fossil WSOC fraction (see Sec. 2.5). Meanwhile,
169 the remaining WSOC fractions are assigned to the secondary factors, which can be from both

170 fossil and non-fossil origins, were considered collectively and compared to the unassigned
171 fossil and non-fossil WSOC, to retrieve the origins of this remaining fraction (see Sec. 2.5).

172

173 2.4 ¹⁴C measurement of WSOC

174 ¹⁴C content of micro-scale WSOC aerosol samples was measured with a newly
175 developed method (Zhang et al., 2014c). Briefly, a 16-mm-diameter punch of each filter was
176 extracted using 10 ml ultrapure water with low TOC impurity (less than 5 ppb). The water
177 extracts were recovered in the 20 ml PFA vials and were then pre-frozen at -20 °C more than 5
178 hours before completely dryness in a freeze dryer (Alpha 2-4 LSC, Christ, Germany) for about
179 24 h to 36 h. The residue was re-dissolved in 50 µl of ultrapure water three times and transferred
180 into 200 µl tin capsules (Elementar, Germany). The concentrated samples were heated in the
181 oven at 55-60 °C until complete dryness before the ¹⁴C measurements.

182 WSOC extracts in tin capsules were then converted to CO₂ by the oxidation of the
183 carbon-containing samples using an Elemental Analyzer (EA, Model Vario Micro, Elementar,
184 Germany) as a combustion unit (up to 1050 °C). The resulting CO₂ was introduced continuously
185 by a versatile gas inlet system into a gas ion source of the accelerator mass spectrometer
186 MICADAS where ¹⁴C of CO₂ was finally measured (Wacker et al., 2013; Salazar et al., 2015).
187 The ¹⁴C content of OC and EC was measured in our previous study (Zhang et al., 2015b). ¹⁴C
188 results were expressed as fraction of modern (f_M), i.e., the fraction of the measured ¹⁴C/¹²C ratio
189 related to the ¹⁴C/¹²C ratio of the reference year 1950 (Stuiver, 1977). To correct excess ¹⁴C
190 from nuclear bomb tests in the 1950s and 1960s, f_M values were converted to the fraction of
191 non-fossil (f_{NF}) (Zotter et al., 2014a; Zhang et al., 2012):

$$192 \quad f_{NF} = f_M / f_{M,ref} \text{ (Eq. 3)}$$

193 $f_{M,ref}$ is a reference value of f_M for non-fossil carbon sources including biogenic and
194 biomass burning emissions, which were estimated as 1.08 ± 0.05 (i.e., $f_{M,ref} = (0.5 * 1.10 + 0.5 * 1.05)$)

195 (see details in (Zhang et al., 2012)) for WSOC samples collected in 2013 according to the
196 contemporary atmospheric CO₂ f_M (Levin et al., 2010) and a tree growth model (Mohn et al.,
197 2008).

198 2.5 AMS²-based source apportionment of WSOC

199 To better understand the origin of WSOC observed at these sites, WSOC sources were
200 apportioned into several major sources by a combination of ¹⁴C and PMF source
201 apportionments (See Figure 1). Here, two “AMS” (i.e., accelerator mass spectrometer and
202 aerosol mass spectrometer), such a combined approach was named as “AMS²-based source
203 apportionment.

204 WSOC concentration from non-fossil (WSOC_{NF}) and fossil (WSOC_F) sources were
205 calculated from:

$$206 \quad \text{WSOC}_{\text{NF}} = \text{WSOC} * f_{\text{NF}}(\text{WSOC}) \text{ (Eq. 4)}$$

$$207 \quad \text{WSOC}_{\text{F}} = \text{WSOC} - \text{WSOC}_{\text{NF}} \text{ (Eq. 5)}$$

208 The mass concentration of WSOC was derived from the subtraction of TC mass
209 measured from a water-extracted filter from that measured with an un-treated filter (Zhang et
210 al., 2012):

$$211 \quad \text{WSOC} = \text{TC}_{\text{un-treated}} - \text{TC}_{\text{water-extracted}} \text{ (Eq.6)}$$

212 Based on mass balance, WIOC concentrations from non-fossil (WIOC_{NF}) and fossil
213 (WIOC_F) sources were calculated from:

$$214 \quad \text{WIOC}_{\text{NF}} = \text{OC}_{\text{NF}} - \text{WSOC}_{\text{NF}} \text{ (Eq. 7)}$$

$$215 \quad \text{WIOC}_{\text{F}} = \text{OC}_{\text{F}} - \text{WSOC}_{\text{F}} \text{ (Eq.8)}$$

216 where OC concentrations from non-fossil (OC_{NF}) and fossil (OC_F) sources were
217 obtained by mass and ^{14}C measurement of the OC fraction, which were reported previously
218 (Zhang et al., 2015b).

219 The non-fossil and fossil-fuel derived WSOC can be apportioned into primary and
220 secondary OC:

$$221 \quad WSOC_{NF} = WSOC_{POC,NF} + WSOC_{SOC,NF} \text{ (Eq.9)}$$

$$222 \quad WSOC_F = WSOC_{POC,F} + WSOC_{SOC,F} \text{ (Eq.10)}$$

223 $WSOC_{POC,NF}$ can be sub-divided into the following three major primary emissions including
224 cooking emission ($WSOC_{CI}$) and biomass burning ($WSOC_{BB}$).

$$225 \quad WSOC_{POC,NF} = WSOC_{CI} + WSOC_{BB} \text{ (Eq.11)}$$

226 Similarly, $WSOC_{POC,F}$ can be sub-divided into the following two major primary emissions
227 including traffic ($WSOC_{TR}$) and coal combustion ($WSOC_{CB}$).

$$228 \quad WSOC_{POC,F} = WSOC_{TR} + WSOC_{CB} \text{ (Eq.12)}$$

229 where primary fractions such as $WSOC_{CI}$, $WSOC_{BB}$, $WSOC_{TR}$ and $WSOC_{CB}$ are
230 previously estimated by the off-line AMS-PMF approach (Huang et al., 2014; Daellenbach et
231 al., 2016; Bozzetti et al., 2017a; Bozzetti et al., 2017b).

232 An uncertainty propagation scheme using a Latin-hypercube sampling (LHS) model
233 was implemented to properly estimate overall uncertainties including measurement
234 uncertainties of the mass determinations of carbon species (i.e., OC, EC, TC, WSOC, WIOC)
235 and ^{14}C measurement, blank corrections from field blanks, and estimation of $f_{M,ref}$ (Zhang et al.,
236 2015b).

237 **3 RESULTS AND DISCUSSION**

238 **3.1 Overall results**

239 During the haze periods of January 2013, the highest daily average PM_{2.5} concentrations were
240 found in Xi'an (345 µg/m³) followed by Beijing (158 µg/m³), Shanghai (90 µg/m³) and
241 Guangzhou (68 µg/m³). These levels were much higher than the China's National ambient Air
242 quality standards (i.e., 35 µg/m³). Indeed, several studies have already reported the chemical
243 composition, source and formation mechanism of PM_{2.5} in many large cities during the haze
244 events of January 2013 in East China. For examples, Huang et al. (2014) revealed that the
245 secondary aerosol formation contributed to 44–71% of OA in Beijing, Xi'an, Shanghai, and
246 Guangzhou during this extremely haze event in China (Huang et al., 2014). By ¹⁴C-based source
247 appointment conducted in the same campaign, Zhang et al. (2015) have reported that
248 carbonaceous aerosol pollution was driven to a large (often dominant) extent by SOA formation
249 from both, fossil and biomass-burning sources (Zhang et al., 2015b). For all four cities, the 24 h
250 average levels of WSOC were significantly correlated with the levels of PM_{2.5} and OC ($R=0.99$,
251 $p<0.01$, Figure 2), suggesting that WSOC and OA may have similar sources and formation
252 processes and thus have important implications for OC loadings and associated environmental
253 and health effects. However, the sources of WSOC remain poorly constrained. In this study,
254 we measured the ¹⁴C content of WSOC aerosols in six samples (three with the highest, three
255 with average PM mass) for each city to report on heavily and moderately polluted days (HPD
256 and MPD, respectively) (Zhang et al., 2015b). The ¹⁴C contents of OC and EC of the same
257 samples were reported previously (Zhang et al., 2015b).

258 WSOC on average accounted for 53±8.0% (ranging from 40-65%) of OC including all samples
259 from the four sites, which was consistent with previous estimates . Based on these
260 measurements, the concentrations of WSOC from non-fossil sources (WSOC_{NF}) spanned from
261 1.41 to 45.3 µg/m³ with a mean of 10.6±12.1 µg/m³, whereas the corresponding range for
262 WSOC from fossil-fuel emissions (WSOC_F) was 0.44 to 20.1 µg/m³ with a mean of 5.3±4.9
263 µg/m³ (Figure 3). Similar to PM_{2.5} levels, the highest concentrations of WSOC_{NF} and WSOC_F
264 were observed in Northern China in Xi'an and Beijing (Xi'an>Beijing), followed by the two
265 southern sites Shanghai and Guangzhou. Non-fossil contributions (mean ± standard deviation)

266 to total WSOC were $53\pm 5\%$, $75\pm 4\%$, $48\pm 2\%$ and $68\pm 6\%$ in Beijing, Xi'an, Shanghai, and
267 Guangzhou, respectively. Thus, fossil contributions were notably higher in Beijing and
268 Shanghai than those in Xi'an and Guangzhou. Such a trend was also observed for OC (Zhang
269 et al., 2015b), suggesting relatively high contribution from fossil-fuel emissions to OC and
270 WSOC due to large coal usage. Despite of these fossil emissions, non-fossil sources were
271 considerably important or even dominant contributors for all the studied sites, which may be
272 associated with primary and secondary OA from regional-transported and local biomass
273 burning emissions. As shown in Figure 4, non-fossil WSOC was significantly correlated with
274 levoglucosan, indicating that a large fraction of non-fossil WSOC was indeed from biomass
275 burning emissions. In addition, no significant or only a negative correlation (Figure 4) was
276 found between levoglucosan and fraction of fossil to WSOC, suggesting that fossil-fuel source
277 is very unlikely a major or important contributor of levoglucosan even in the regions (e.g.,
278 Xi'an and Beijing in this study) where coal combustion is important during the cold period
279 (Zhang et al., 2015a). It should also be noted that formation of SOA derived from biogenic
280 VOCs may also have contributed to $WSOC_{NF}$ in Guangzhou, where temperatures during the
281 sampling period were significantly higher (i.e., $5-18\text{ }^{\circ}\text{C}$) than those in other cities (i.e., -12 to
282 $+9\text{ }^{\circ}\text{C}$) (Bozzetti et al., 2017b). Although both fossil and non-fossil WSOC concentrations were
283 dramatically enhanced during HPD compared to those during MPD, their relative contributions
284 did not change significantly in Beijing and Shanghai whereas a small increasing and decreasing
285 trend in non-fossil fraction was found in Xi'an and Guangzhou, respectively (Figure 3). This
286 suggests that the source pattern of WSOC in Beijing and Shanghai remained similar between
287 HPD and MPD, but the increase in the WSOC concentrations was rather enhanced by additional
288 fossil-fuel and biogenic/biomass burning emissions in Guangzhou and Xi'an, respectively. It
289 should be noted that the meteorological conditions play significant roles on the haze formation
290 in the eastern China during winter 2013, and has already been well documented (Zhang et al.,
291 2014a). However, the details sources of WSOC and WIOC were still unclear.

292 3.2 WSOC versus WIOC

293 To compare sources of WSOC and WIOC aerosols, the mass concentrations and ^{14}C contents
294 of WIOC were also derived based on mass balance. The ^{14}C -based source apportionment of
295 WIOC and the relationship between $f_{\text{NF}}(\text{WSOC})$ and $f_{\text{NF}}(\text{WIOC})$ is presented in Figures 5 and
296 6a, respectively. It shows that non-fossil contributions to WSOC were larger than those of
297 WIOC for nearly all samples in Beijing, Xi'an and Guangzhou. On average, the majority (60-
298 70%) of the fossil OC was water insoluble at these 3 sites (see Figure 6b), indicating that fossil-
299 derived OA mostly consisted of hydrophobic components and thus is less water soluble than
300 OA from non-fossil sources. This result is consistent with findings reported elsewhere such as
301 at an urban or rural site in Switzerland (Zhang et al., 2013), a remote site in Hainan Island,
302 South China (Zhang et al., 2014b) and at two rural sites on the east coast of the United States
303 (Wozniak et al., 2012). Meanwhile, the fossil OC in Shanghai, the dominant fraction of OC,
304 was more water soluble (Figure 6b), suggesting an enhanced SOA formation from fossil VOCs
305 from vehicle emissions and/or coal burning for this city. As shown in Figure 6b, non-fossil OA
306 was enriched in water-soluble fractions (i.e., $60\% \pm 8\%$) for all cities, associated with the
307 hydrophilic properties of biogenic-derived SOA and biomass-burning derived primary organic
308 aerosol (POA) and SOA, which are composed of a large fraction of polar and highly oxygenated
309 compounds (Mayol-Bracero et al., 2002; Sullivan et al., 2011; Noziere et al., 2015). Thus, non-
310 fossil OC has more water-soluble components than fossil ones. It should be noted that relative
311 contributions of WSOC_{NF} and WSOC_{F} are similar in Beijing and Shanghai, whereas WSOC_{NF}
312 is much higher than WSOC_{F} in Xi'an and Guangzhou. This suggests larger contribution of non-
313 fossil sources to WSOC aerosols in Xi'an and Guangzhou than those in Beijing and Shanghai.

314 **3.3 High contribution of secondary formation to WSOC**

315 WSOC was further apportioned into fossil sources such as coal burning (CB), traffic (TR) and
316 SOC (SOC,F) as well as non-fossil sources such as biomass burning (BB), cooking (CI) and
317 SOC (SOC,NF) using a AMS² based source apportionment (see Sec. 2.5 and Figure 1). SOC
318 dominated WSOC during both the HPD and MPD with a mean contribution of $67\% \pm 9\%$,
319 highlighting the importance of SOC formation to the WSOC aerosols in wintertime pollution

320 events. This is consistent with our previous findings for total PM_{2.5} mass and bulk carbonaceous
321 aerosols (i.e., total carbon, sum of OC and EC) (Huang et al., 2014; Zhang et al., 2015b). The
322 increase in SOC contribution to WSOC during HPD compared to MPD can be largely due to
323 fossil contribution in Beijing but non-fossil emissions in Xi'an. In Shanghai and Guangzhou,
324 the source pattern of WSOC was not significantly different between MPD and HPD. Fossil
325 contributions to WSOC_{SOC} were 50%±9% in Beijing, 61±4% in Shanghai, associated with SOA
326 from local and transported fossil-fuel derived precursors at these sites (Guo et al., 2014). This
327 contribution drops to 36±9% and 26±9% in Guangzhou and Xi'an, respectively, due to higher
328 biomass-burning contribution to SOC. Despite of the general importance of fossil SOC,
329 formation of non-fossil WSOC_{SOC} becomes especially relevant during HPD especially in Xi'an
330 (Figure 7), which may be explained by competing effects in SOC formation from fossil versus
331 non-fossil precursors. It can be hypothesized for extremely polluted episodes that more
332 hydrophilic volatile compounds that were emitted from biomass burning precursors
333 preferentially form SOC compounds via heterogeneous reaction/processing on dust particles
334 compared to highly hydrophobic precursors from fossil sources, a point subjected to future
335 laboratory and field experiments. The most important primary sources of WSOC were biomass
336 burning emissions, and their contributions were higher in Xi'an (26%±7%) and Guangzhou
337 (25%±6%) than those found in Beijing (17%±6%) and Shanghai (17%±5%). The remaining
338 primary sources such as coal combustion, cooking and traffic were generally very small
339 contributors of WSOC due to lower water solubility, although coal combustion could exceed
340 10% in Beijing. It should be noted that WSOC was dominated by SOC formation with mean
341 contribution of 61%±10% and 72%±12% (average for all four cities) to non-fossil and fossil-
342 fuel derived WSOC, respectively.

343 **Summary and implications**

344 Our study demonstrates that non-fossil emissions are generally a dominant contributor of
345 WSOC aerosols during extreme haze events in representative major cities of China, which is in
346 agreement with WSOC source information identified in aerosols with different size fractions

347 (e.g., TSP, PM₁₀ and PM_{2.5}) observed in the Northern Hemisphere at urban, rural, semi-urban,
348 and background sites in East/South Asia, Europe and USA (Table 1). The ¹⁴C-based source
349 apportionment database shows a mean non-fossil fraction of 73±11% across all sites. This
350 overwhelming non-fossil contribution to WSOC is consistently observed throughout the year,
351 which is associated with seasonal-dependent biomass-burning emissions and/or biogenic-
352 derived SOC formation. Our study provides evidence that the presence of oxidized OA, which
353 is to a large extent water soluble, in the Northern Hemisphere (Zhang et al., 2007) is mainly
354 derived from biogenic-derived SOA and/or biomass burning sources. The overall importance
355 of non-fossil emissions to the WSOC aerosols results from large contributions of SOC
356 formation from biogenic precursors (e.g., most likely during summer) and relatively high water-
357 solubility of primary biomass burning particles (e.g., most likely during winter) compared to
358 those emitted from fossil fuel emissions such as coal combustion and vehicle exhaust. Despite
359 of the importance of non-fossil sources, a significant fossil fraction is also observed in the
360 WSOC aerosols from polluted regions in East Asia and sites influenced by East Asian
361 continental outflow (Table 1, Figure 8). This fossil contribution is apparently higher than in this
362 region than in the USA and Europe, which is due to large industrial and residential coal usage
363 as well as vehicle emissions. From our observation, the increases in the fossil fractions of
364 WSOC were mostly from SOC formation. Since WSOC has hygroscopic properties, our
365 findings suggest that SOC formation from non-fossil emissions have significant implications
366 on aerosol-induced climate effects. In addition, fossil-derived SOC formation may also become
367 important in polluted regions with large amounts of fossil fuel emissions such as in China and
368 other emerging countries. Low combustion efficiencies and consequently high emission factors
369 in most of the combustion processes in China may further be responsible for increased
370 concentrations of fossil precursors which may be oxidized to form water-soluble SOA in the
371 atmosphere and contribute substantially to the WSOC aerosols. The enhanced WSOC levels
372 may be also originate from aging of fossil POA during the long-range transport of aerosols
373 (Kirillova et al., 2014a). It is also interesting to note that fossil contribution during winter in
374 East Asia is generally higher than those in the rest of the year although relatively large fossil

375 fraction could be occasionally found as well. Such seasonal dependence was not observed in
376 other regions, suggesting the importance of fossil contribution to WSOC due to increasing coal
377 combustions during winter in China. This study provides a more detailed source apportionment
378 of WSOC, which could improve modelling of climate and health effects as well as the
379 understanding of atmospheric chemistry of WSOC in the polluted atmosphere such as China
380 and provide scientific basis for policy decisions on air pollution emissions mitigation.

381 REFERENCES

382 Andreae, M. O., and Gelencser, A.: Black carbon or brown carbon? The nature of light-
383 absorbing carbonaceous aerosols, *Atmos. Chem. Phys.*, 6, 3131-3148, 2006.

384 Asa-Awuku, A., Moore, R. H., Nenes, A., Bahreini, R., Holloway, J. S., Brock, C. A.,
385 Middlebrook, A. M., Ryerson, T. B., Jimenez, J. L., DeCarlo, P. F., Hecobian, A., Weber, R.
386 J., Stickel, R., Tanner, D. J., and Huey, L. G.: Airborne cloud condensation nuclei
387 measurements during the 2006 Texas Air Quality Study, *J. Geophys. Res.*, 116, D11201,
388 doi:10.1029/2010jd014874, 2011.

389 Bosch, C., Andersson, A., Kirillova, E. N., Budhavant, K., Tiwari, S., Praveen, P. S., Russell,
390 L. M., Beres, N. D., Ramanathan, V., and Gustafsson, O.: Source-diagnostic dual-isotope
391 composition and optical properties of water-soluble organic carbon and elemental carbon in the
392 South Asian outflow intercepted over the Indian Ocean, *J. Geophys. Res.*, 119, 11743-11759,
393 doi:10.1002/2014JD022127, 2014.

394 Bozzetti, C., El Haddad, I., Salameh, D., Daellenbach, K. R., Fermo, P., Gonzalez, R.,
395 Minguillón, M. C., Iinuma, Y., Poulain, L., Elser, M., Müller, E., Slowik, J. G., Jaffrezo, J. L.,
396 Baltensperger, U., Marchand, N., and Prévôt, A. S. H.: Organic aerosol source apportionment
397 by offline-AMS over a full year in Marseille, *Atmos. Chem. Phys.*, 17, 8247-8268,
398 doi:10.5194/acp-17-8247-2017, 2017a.

399 Bozzetti, C., Sosedova, Y., Xiao, M., Daellenbach, K. R., Ulevicius, V., Dudoitis, V., Mordas,
400 G., Byčenkienė, S., Plauškaitė, K., Vlachou, A., Golly, B., Chazeau, B., Besombes, J. L.,
401 Baltensperger, U., Jaffrezo, J. L., Slowik, J. G., El Haddad, I., and Prévôt, A. S. H.: Argon

402 offline-AMS source apportionment of organic aerosol over yearly cycles for an urban, rural,
403 and marine site in northern Europe, *Atmos. Chem. Phys.*, 17, 117-141, doi:10.5194/acp-17-
404 117-2017, 2017b.

405 Canonaco, F., Crippa, M., Slowik, J. G., Baltensperger, U., and Prévôt, A. S. H.: SoFi, an
406 IGOR-based interface for the efficient use of the generalized multilinear engine (ME-2) for the
407 source apportionment: ME-2 application to aerosol mass spectrometer data, *Atmos. Meas.*
408 *Tech.*, 6, 3649-3661, doi:10.5194/amt-6-3649-2013, 2013.

409 Cao, F., Zhang, Y.-L., Szidat, S., Zapf, A., Wacker, L., and Schwikowski, M.: Microgram-level
410 radiocarbon determination of carbonaceous particles in firn and ice samples: pretreatment and
411 OC/EC separation, *Radiocarbon*, 55, 383-390, 2013.

412 Cao, F., Zhang, Y., Ren, L., Liu, J., Li, J., Zhang, G., Liu, D., Sun, Y., Wang, Z., Shi, Z., and
413 Fu, P.: New insights into the sources and formation of carbonaceous aerosols in China: potential
414 applications of dual-carbon isotopes, *National Science Review*, nwx097-nwx097,
415 doi:10.1093/nsr/nwx097, 2017.

416 Cavalli, F., Viana, M., Yttri, K. E., Genberg, J., and Putaud, J. P.: Toward a standardised
417 thermal-optical protocol for measuring atmospheric organic and elemental carbon: the
418 EUSAAR protocol, *Atmos. Meas. Tech.*, 3, 79-89, 2010.

419 Cheng, Y., He, K. B., Zheng, M., Duan, F. K., Du, Z. Y., Ma, Y. L., Tan, J. H., Yang, F. M.,
420 Liu, J. M., Zhang, X. L., Weber, R. J., Bergin, M. H., and Russell, A. G.: Mass absorption
421 efficiency of elemental carbon and water-soluble organic carbon in Beijing, China, *Atmos.*
422 *Chem. Phys.*, 11, 11497-11510, doi:10.5194/acp-11-11497-2011, 2011.

423 Daellenbach, K. R., Bozzetti, C., Krepeleva, A. K., Canonaco, F., Wolf, R., Zotter, P., Fermo,
424 P., Crippa, M., Slowik, J. G., Sosedova, Y., Zhang, Y., Huang, R. J., Poulain, L., Szidat, S.,
425 Baltensperger, U., El Haddad, I., and Prevot, A. S. H.: Characterization and source
426 apportionment of organic aerosol using offline aerosol mass spectrometry, *Atmos. Meas. Tech.*,
427 9, 23-39, doi:10.5194/amt-9-23-2016, 2016.

428 Dusek, U., Hitzenberger, R., Kasper-Giebl, A., Kistler, M., Meijer, H. A. J., Szidat, S., Wacker,
429 L., Holzinger, R., and Röckmann, T.: Sources and formation mechanisms of carbonaceous

430 aerosol at a regional background site in the Netherlands: insights from a year-long radiocarbon
431 study, *Atmos. Chem. Phys.*, 17, 3233-3251, doi:10.5194/acp-17-3233-2017, 2017.

432 Fang, W., Andersson, A., Zheng, M., Lee, M., Holmstrand, H., Kim, S.-W., Du, K., and
433 Gustafsson, Ö.: Divergent Evolution of Carbonaceous Aerosols during Dispersal of East Asian
434 Haze, *Scientific Reports*, 7, 10422, doi:10.1038/s41598-017-10766-4, 2017.

435 Fu, P., Kawamura, K., Chen, J., Qin, M., Ren, L., Sun, Y., Wang, Z., Barrie, L. A., Tachibana,
436 E., Ding, A., and Yamashita, Y.: Fluorescent water-soluble organic aerosols in the High Arctic
437 atmosphere, *Sci Rep*, 5, 9845, doi:10.1038/srep09845, 2015.

438 Guo, S., Hu, M., Zamora, M. L., Peng, J., Shang, D., Zheng, J., Du, Z., Wu, Z., Shao, M., Zeng,
439 L., Molina, M. J., and Zhang, R.: Elucidating severe urban haze formation in China, *Proc. Nat.
440 Acad. Sci. U.S.A.*, 111, 17373-17378, doi:10.1073/pnas.1419604111, 2014.

441 Hecobian, A., Zhang, X., Zheng, M., Frank, N., Edgerton, E. S., and Weber, R. J.: Water-
442 Soluble Organic Aerosol material and the light-absorption characteristics of aqueous extracts
443 measured over the Southeastern United States, *Atmos. Chem. Phys.*, 10, 5965-5977,
444 doi:10.5194/acp-10-5965-2010, 2010.

445 Huang, R. J., Zhang, Y., Bozzetti, C., Ho, K. F., Cao, J. J., Han, Y., Daellenbach, K. R., Slowik,
446 J. G., Platt, S. M., Canonaco, F., Zotter, P., Wolf, R., Pieber, S. M., Bruns, E. A., Crippa, M.,
447 Ciarelli, G., Piazzalunga, A., Schwikowski, M., Abbaszade, G., Schnelle-Kreis, J.,
448 Zimmermann, R., An, Z., Szidat, S., Baltensperger, U., El Haddad, I., and Prevot, A. S.: High
449 secondary aerosol contribution to particulate pollution during haze events in China, *Nature*, 514,
450 218-222, doi:10.1038/nature13774, 2014.

451 Jimenez, J. L., Canagaratna, M. R., Donahue, N. M., Prevot, A. S. H., Zhang, Q., Kroll, J. H.,
452 DeCarlo, P. F., Allan, J. D., Coe, H., Ng, N. L., Aiken, A. C., Docherty, K. S., Ulbrich, I. M.,
453 Grieshop, A. P., Robinson, A. L., Duplissy, J., Smith, J. D., Wilson, K. R., Lanz, V. A., Hueglin,
454 C., Sun, Y. L., Tian, J., Laaksonen, A., Raatikainen, T., Rautiainen, J., Vaattovaara, P., Ehn,
455 M., Kulmala, M., Tomlinson, J. M., Collins, D. R., Cubison, M. J., Dunlea, E. J., Huffman, J.
456 A., Onasch, T. B., Alfarra, M. R., Williams, P. I., Bower, K., Kondo, Y., Schneider, J.,
457 Drewnick, F., Borrmann, S., Weimer, S., Demerjian, K., Salcedo, D., Cottrell, L., Griffin, R.,

458 Takami, A., Miyoshi, T., Hatakeyama, S., Shimono, A., Sun, J. Y., Zhang, Y. M., Dzepina, K.,
459 Kimmel, J. R., Sueper, D., Jayne, J. T., Herndon, S. C., Trimborn, A. M., Williams, L. R., Wood,
460 E. C., Middlebrook, A. M., Kolb, C. E., Baltensperger, U., and Worsnop, D. R.: Evolution of
461 organic aerosols in the atmosphere, *Science*, 326, 1525-1529, doi:DOI
462 10.1126/science.1180353, 2009.

463 Kirillova, E. N., Sheesley, R. J., Andersson, A., and Gustafsson, O.: Natural abundance ^{13}C and
464 ^{14}C analysis of water-soluble organic carbon in atmospheric aerosols, *Anal. Chem.*, 82, 7973-
465 7978, doi:Doi 10.1021/Ac1014436, 2010.

466 Kirillova, E. N., Andersson, A., Sheesley, R. J., Kruså, M., Praveen, P. S., Budhavant, K., Safai,
467 P. D., Rao, P. S. P., and Gustafsson, Ö.: ^{13}C and ^{14}C -based study of sources and atmospheric
468 processing of water-soluble organic carbon (WSOC) in South Asian aerosols, *J. Geophys. Res.*,
469 118, 614-626, doi:10.1002/jgrd.50130, 2013.

470 Kirillova, E. N., Andersson, A., Han, J., Lee, M., and Gustafsson, O.: Sources and light
471 absorption of water-soluble organic carbon aerosols in the outflow from northern China, *Atmos.*
472 *Chem. Phys.*, 14, 1413-1422, doi:DOI 10.5194/acp-14-1413-2014, 2014a.

473 Kirillova, E. N., Andersson, A., Tiwari, S., Srivastava, A. K., Bisht, D. S., and Gustafsson, O.:
474 Water-soluble organic carbon aerosols during a full New Delhi winter: Isotope-based source
475 apportionment and optical properties, *J. Geophys. Res.*, 119, 3476-3485, doi:Doi
476 10.1002/2013jd020041, 2014b.

477 Kondo, Y., Miyazaki, Y., Takegawa, N., Miyakawa, T., Weber, R. J., Jimenez, J. L., Zhang,
478 Q., and Worsnop, D. R.: Oxygenated and water-soluble organic aerosols in Tokyo, *J. Geophys.*
479 *Res.*, 112, D01203, doi:10.1029/2006jd007056, 2007.

480 Laskin, A., Laskin, J., and Nizkorodov, S. A.: Chemistry of Atmospheric Brown Carbon, *Chem.*
481 *Rev. (Washington, DC, U. S.)*, 115, 4335-4382, doi:10.1021/cr5006167, 2015.

482 Levin, I., Naegler, T., Kromer, B., Diehl, M., Francey, R. J., Gomez-Pelaez, A. J., Steele, L. P.,
483 Wagenbach, D., Weller, R., and Worthy, D. E.: Observations and modelling of the global
484 distribution and long-term trend of atmospheric $^{14}\text{CO}_2$, *Tellus B*, 62, 26-46,
485 doi:10.1111/j.1600-0889.2009.00446.x, 2010.

486 Limbeck, A., Handler, M., Neuberger, B., Klatzer, B., and Puxbaum, H.: Carbon-specific
487 analysis of humic-like substances in atmospheric aerosol and precipitation samples, *Anal.*
488 *Chem.*, 77, 7288-7293, doi:10.1021/ac0509531, 2005.

489 Liu, J., Li, J., Vonwiller, M., Liu, D., Cheng, H., Shen, K., Salazar, G., Agrios, K., Zhang, Y.,
490 He, Q., Ding, X., Zhong, G., Wang, X., Szidat, S., and Zhang, G.: The importance of non-fossil
491 sources in carbonaceous aerosols in a megacity of central China during the 2013 winter haze
492 episode: A source apportionment constrained by radiocarbon and organic tracers, *Atmos.*
493 *Environ.*, 144, 60-68, doi:<http://dx.doi.org/10.1016/j.atmosenv.2016.08.068>, 2016.

494 Liu, J. W., Li, J., Zhang, Y. L., Liu, D., Ding, P., Shen, C. D., Shen, K. J., He, Q. F., Ding, X.,
495 Wang, X. M., Chen, D. H., Szidat, S., and Zhang, G.: Source Apportionment Using
496 Radiocarbon and Organic Tracers for PM_{2.5} Carbonaceous Aerosols in Guangzhou, South
497 China: Contrasting Local- and Regional-Scale Haze Events, *Environ. Sci. Technol.*, 48, 12002-
498 12011, doi:Doi 10.1021/Es503102w, 2014.

499 Mayol-Bracero, O. L., Guyon, P., Graham, B., Roberts, G., Andreae, M. O., Decesari, S.,
500 Facchini, M. C., Fuzzi, S., and Artaxo, P.: Water-soluble organic compounds in biomass
501 burning aerosols over Amazonia - 2. Apportionment of the chemical composition and
502 importance of the polyacidic fraction, *J. Geophys. Res.*, 107, D8091,
503 doi:10.1029/2001jd000522, 2002.

504 Miyazaki, Y., Kondo, Y., Takegawa, N., Komazaki, Y., Fukuda, M., Kawamura, K., Mochida,
505 M., Okuzawa, K., and Weber, R. J.: Time-resolved measurements of water-soluble organic
506 carbon in Tokyo, *J. Geophys. Res.*, 111, D23206, doi:1029/2006jd007125, 2006.

507 Mohn, J., Szidat, S., Fellner, J., Rechberger, H., Quartier, R., Buchmann, B., and Emmenegger,
508 L.: Determination of biogenic and fossil CO₂ emitted by waste incineration based on ¹⁴CO₂ and
509 mass balances, *Bioresour. Technol.*, 99, 6471-6479, doi:DOI 10.1016/j.biortech.2007.11.042,
510 2008.

511 Noziere, B., Kalberer, M., Claeys, M., Allan, J., D'Anna, B., Decesari, S., Finessi, E., Glasius,
512 M., Grgic, I., Hamilton, J. F., Hoffmann, T., Iinuma, Y., Jaoui, M., Kahnt, A., Kampf, C. J.,
513 Kourtchev, I., Maenhaut, W., Marsden, N., Saarikoski, S., Schnelle-Kreis, J., Surratt, J. D.,

514 Szidat, S., Szmigielski, R., and Wisthaler, A.: The molecular identification of organic
515 compounds in the atmosphere: state of the art and challenges, *Chem Rev*, 115, 3919-3983,
516 doi:10.1021/cr5003485, 2015.

517 Pavuluri, C. M., Kawamura, K., Uchida, M., Kondo, M., and Fu, P. Q.: Enhanced modern
518 carbon and biogenic organic tracers in Northeast Asian aerosols during spring/summer, *J.*
519 *Geophys. Res.*, 118, 2362-2371, doi:Doi 10.1002/Jgrd.50244, 2013.

520 Ruellan, S., and Cachier, H.: Characterisation of fresh particulate vehicular exhausts near a
521 Paris high flow road, *Atmos. Environ.*, 35, 453-468, doi:Doi 10.1016/S1352-2310(00)00110-
522 2, 2001.

523 Salazar, G., Zhang, Y. L., Agrios, K., and Szidat, S.: Development of a method for fast and
524 automatic radiocarbon measurement of aerosol samples by online coupling of an elemental
525 analyzer with a MICADAS AMS, *Nucl. Instr. and Meth. in Phys. Res. B.*, 361, 163-167,
526 doi:<http://dx.doi.org/10.1016/j.nimb.2015.03.051>, 2015.

527 Sannigrahi, P., Sullivan, A. P., Weber, R. J., and Ingall, E. D.: Characterization of water-soluble
528 organic carbon in urban atmospheric aerosols using solid-state C-13 NMR spectroscopy,
529 *Environ. Sci. Technol.*, 40, 666-672, doi:Doi 10.1021/Es051150i, 2006.

530 Stuiver, M.: Discussion: Reporting of ¹⁴C data, *Radiocarbon*, 19, 355-363, 1977.

531 Sullivan, A. P., Frank, N., Kenski, D. M., and Collett, J. L.: Application of high-performance
532 anion-exchange chromatography-pulsed amperometric detection for measuring carbohydrates
533 in routine daily filter samples collected by a national network: 2. Examination of sugar
534 alcohols/polyols, sugars, and anhydrosugars in the upper Midwest, *J. Geophys. Res.*, 116,
535 D08303, doi:10.1029/2010jd014169, 2011.

536 Szidat, S., Jenk, T. M., Gäggeler, H. W., Synal, H. A., Fisseha, R., Baltensperger, U., Kalberer,
537 M., Samburova, V., Wacker, L., Saurer, M., Schwikowski, M., and Hajdas, I.: Source
538 apportionment of aerosols by ¹⁴C measurements in different carbonaceous particle fractions,
539 *Radiocarbon*, 46, 475-484, 2004.

540 Szidat, S., Ruff, M., Perron, N., Wacker, L., Synal, H.-A., Hallquist, M., Shannigrahi, A. S.,
541 Yttri, K. E., Dye, C., and Simpson, D.: Fossil and non-fossil sources of organic carbon (OC)
542 and elemental carbon (EC) in Goeteborg, Sweden, *Atmos. Chem. Phys.*, 9, 1521-1535, 2009.

543 Timonen, H., Carbone, S., Aurela, M., Saarnio, K., Saarikoski, S., Ng, N. L., Canagaratna, M.
544 R., Kulmala, M., Kerminen, V. M., Worsnop, D. R., and Hillamo, R.: Characteristics, sources
545 and water-solubility of ambient submicron organic aerosol in springtime in Helsinki, Finland,
546 *J. Aerosol Sci.*, 56, 61-77, doi:10.1016/j.jaerosci.2012.06.005, 2013.

547 Wacker, L., Fahrni, S. M., Hajdas, I., Molnar, M., Synal, H. A., Szidat, S., and Zhang, Y. L.: A
548 versatile gas interface for routine radiocarbon analysis with a gas ion source, *Nucl. Instrum.*
549 *Meth. B*, 294, 315-319, doi:DOI 10.1016/j.nimb.2012.02.009, 2013.

550 Weber, R. J., Sullivan, A. P., Peltier, R. E., Russell, A., Yan, B., Zheng, M., de Gouw, J.,
551 Warneke, C., Brock, C., Holloway, J. S., Atlas, E. L., and Edgerton, E.: A study of secondary
552 organic aerosol formation in the anthropogenic-influenced southeastern United States, *J.*
553 *Geophys. Res.*, 112, D13302, doi:10.1029/2007jd008408, 2007.

554 Wozniak, A. S., Bauer, J. E., and Dickhut, R. M.: Characteristics of water-soluble organic
555 carbon associated with aerosol particles in the eastern United States, *Atmos. Environ.*, 46, 181-
556 188, doi:DOI 10.1016/j.atmosenv.2011.10.001, 2012.

557 Xiao, R., Takegawa, N., Zheng, M., Kondo, Y., Miyazaki, Y., Miyakawa, T., Hu, M., Shao, M.,
558 Zeng, L., Gong, Y., Lu, K., Deng, Z., Zhao, Y., and Zhang, Y. H.: Characterization and source
559 apportionment of submicron aerosol with aerosol mass spectrometer during the PRIDE-PRD
560 2006 campaign, *Atmos. Chem. Phys.*, 11, 6911-6929, doi:10.5194/acp-11-6911-2011, 2011.

561 Yan, C., Zheng, M., Bosch, C., Andersson, A., Desyaterik, Y., Sullivan, A. P., Collett, J. L.,
562 Zhao, B., Wang, S., He, K., and Gustafsson, O.: Important fossil source contribution to brown
563 carbon in Beijing during winter, *Sci Rep*, 7, 43182, doi:10.1038/srep43182, 2017.

564 Zappoli, S., Andracchio, A., Fuzzi, S., Facchini, M. C., Gelencser, A., Kiss, G., Krivacsy, Z.,
565 Molnar, A., Meszaros, E., Hansson, H. C., Rosman, K., and Zebuhr, Y.: Inorganic, organic and
566 macromolecular components of fine aerosol in different areas of Europe in relation to their

567 water solubility, *Atmos. Environ.*, 33, 2733-2743, doi:Doi 10.1016/S1352-2310(98)00362-8,
568 1999.

569 Zhang, Q., Jimenez, J. L., Canagaratna, M. R., Allan, J. D., Coe, H., Ulbrich, I., Alfarra, M. R.,
570 Takami, A., Middlebrook, A. M., Sun, Y. L., Dzepina, K., Dunlea, E., Docherty, K., DeCarlo,
571 P. F., Salcedo, D., Onasch, T., Jayne, J. T., Miyoshi, T., Shimo, A., Hatakeyama, S.,
572 Takegawa, N., Kondo, Y., Schneider, J., Drewnick, F., Borrmann, S., Weimer, S., Demerjian,
573 K., Williams, P., Bower, K., Bahreini, R., Cottrell, L., Griffin, R. J., Rautiainen, J., Sun, J. Y.,
574 Zhang, Y. M., and Worsnop, D. R.: Ubiquity and dominance of oxygenated species in organic
575 aerosols in anthropogenically-influenced Northern Hemisphere midlatitudes, *Geophys. Res.*
576 *Let.*, 34, L13801, doi:DOI:10.1029/2007gl029979, 2007.

577 Zhang, R., Li, Q., and Zhang, R.: Meteorological conditions for the persistent severe fog and
578 haze event over eastern China in January 2013, *SCIENCE CHINA Earth Sciences*, 57, 26-35,
579 doi:10.1007/s11430-013-4774-3, 2014a.

580 Zhang, Y.-L., Li, J., Zhang, G., Zotter, P., Huang, R.-J., Tang, J.-H., Wacker, L., Prévôt, A. S.
581 H., and Szidat, S.: Radiocarbon-based source apportionment of carbonaceous aerosols at a
582 regional background site on hainan Island, South China, *Environ. Sci. Technol.*, 48, 2651-2659,
583 doi:10.1021/es4050852, 2014b.

584 Zhang, Y.-L., Liu, J.-W., Salazar, G. A., Li, J., Zotter, P., Zhang, G., Shen, R.-r., Schäfer, K.,
585 Schnelle-Kreis, J., Prévôt, A. S. H., and Szidat, S.: Micro-scale (μg) radiocarbon analysis of
586 water-soluble organic carbon in aerosol samples, *Atmos. Environ.*, 97, 1-5,
587 doi:<http://dx.doi.org/10.1016/j.atmosenv.2014.07.059>, 2014c.

588 Zhang, Y.-L., Schnelle-Kreis, J. r., Abbaszade, G. l., Zimmermann, R., Zotter, P., Shen, R.-r.,
589 Schäfer, K., Shao, L., Prévôt, A. S. H., and Szidat, S. n.: Source apportionment of elemental
590 carbon in Beijing, China: Insights from radiocarbon and organic marker measurements,
591 *Environ. Sci. Technol.*, 49, 8408-8415, 2015a.

592 Zhang, Y., Ren, H., Sun, Y., Cao, F., Chang, Y., Liu, S., Lee, X., Agrios, K., Kawamura, K.,
593 Liu, D., Ren, L., Du, W., Wang, Z., Prevot, A. S. H., Szidat, S., and Fu, P.: High Contribution

594 of Nonfossil Sources to Submicrometer Organic Aerosols in Beijing, China, *Environ. Sci.*
595 *Technol.*, 51, 7842-7852, doi:10.1021/acs.est.7b01517, 2017.

596 Zhang, Y. L., Perron, N., Ciobanu, V. G., Zotter, P., Minguillón, M. C., Wacker, L., Prévôt, A.
597 S. H., Baltensperger, U., and Szidat, S.: On the isolation of OC and EC and the optimal strategy
598 of radiocarbon-based source apportionment of carbonaceous aerosols, *Atmos. Chem. Phys.*, 12,
599 10841-10856, 2012.

600 Zhang, Y. L., Zotter, P., Perron, N., Prévôt, A. S. H., Wacker, L., and Szidat, S.: Fossil and
601 non-fossil sources of different carbonaceous fractions in fine and coarse particles by
602 radiocarbon measurement, *Radiocarbon*, 55, 1510-1520, 2013.

603 Zhang, Y. L., Huang, R. J., El Haddad, I., Ho, K. F., Cao, J. J., Han, Y., Zotter, P., Bozzetti, C.,
604 Daellenbach, K. R., Canonaco, F., Slowik, J. G., Salazar, G., Schwikowski, M., Schnelle-Kreis,
605 J., Abbaszade, G., Zimmermann, R., Baltensperger, U., Prévôt, A. S. H., and Szidat, S.: Fossil
606 vs. non-fossil sources of fine carbonaceous aerosols in four Chinese cities during the extreme
607 winter haze episode of 2013, *Atmos. Chem. Phys.*, 15, 1299-1312, doi:10.5194/acp-15-1299-
608 2015, 2015b.

609 Zong, Z., Wang, X., Tian, C., Chen, Y., Han, G., Li, J., and Zhang, G.: Source and formation
610 characteristics of water-soluble organic carbon in the anthropogenic-influenced Yellow River
611 Delta, North China, *Atmos. Environ.*, 144, 124-132,
612 doi:<https://doi.org/10.1016/j.atmosenv.2016.08.078>, 2016.

613 Zotter, P., Ciobanu, V. G., Zhang, Y. L., El-Haddad, I., Macchia, M., Daellenbach, K. R.,
614 Salazar, G. A., Huang, R. J., Wacker, L., Hueglin, C., Piazzalunga, A., Fermo, P., Schwikowski,
615 M., Baltensperger, U., Szidat, S., and Prévôt, A. S. H.: Radiocarbon analysis of elemental and
616 organic carbon in Switzerland during winter-smog episodes from 2008 to 2012 – Part 1: Source
617 apportionment and spatial variability, *Atmos. Chem. Phys.*, 14, 13551-13570, doi:10.5194/acp-
618 14-13551-2014, 2014a.

619 Zotter, P., El-Haddad, I., Zhang, Y., Hayes, P. L., Zhang, X., Lin, Y.-H., Wacker, L., Schnelle-
620 Kreis, J., Abbaszade, G., Zimmermann, R., Surratt, J. D., Weber, R., Jimenez, J. L., Szidat, S.,
621 Baltensperger, U., and Prévôt, A. S. H.: Diurnal cycle of fossil and nonfossil carbon using

622 radiocarbon analyses during CalNex, J. Geophys. Res., 119, 6818-6835,
623 doi:10.1002/2013jd021114, 2014b.

624

625 **Author Contributions:** Y.-L.Z., S.S., R.J.H., J.J.C. and A.S.H.P. designed the study. Y.L.Z.
626 and G.S. perform ^{14}C measurement. Y.L.Z. and S. S. interpreted the ^{14}C data. R.J.H., I.E.H.,
627 C.B. and K.D. performed the offline AMS analysis and interpret the data. Y.-L.Z. and I.E.H.
628 perform ^{14}C -AMS-PMF source apportionments. Y.-L.Z. wrote the paper. All authors reviewed
629 and commented on the paper.

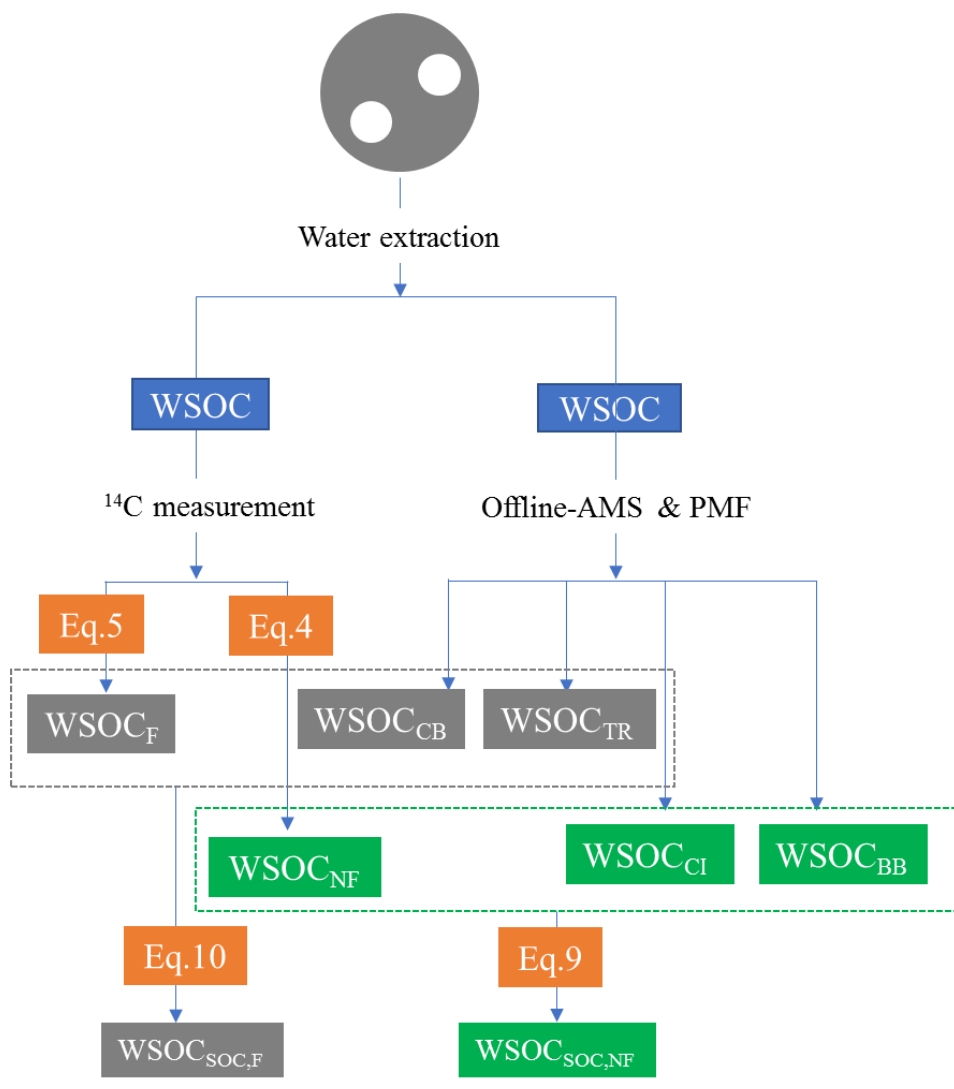
630 **Competing interests:** The authors declare no competing financial interests.

631 **Acknowledgments:** This work was supported by The National Key Research and Development
632 Program of China (Grant No. SQ2017ZY010322-04) and the National Natural Science
633 Foundation of China (Grant Nos. 41603104 and 91644103). All data needed to evaluate the
634 conclusions in the paper are present in the paper. Additional data related to this paper may be
635 requested from the authors.

637 **Table 1.** Compilation of literature values of relative fossil-fuel contributions (fossil %) to the
 638 WSOC aerosols in East/South Asia, USA and Europe.

Site	Location	Season	Size	WSOC ($\mu\text{g}/\text{m}^3$)	WSOC/OC	Fossil %	References
East Asia							
Urban	Beijing, China	Winter/2013	PM _{2.5}	19.8	0.49	47	this work
Urban	Xi'an, China	Winter/2013	PM _{2.5}	31.3	0.53	25	this work
Urban	Shanghai, China	Winter/2013	PM _{2.5}	6.5	0.58	52	this work
Urban	Guangzhou, China	Winter/2013	PM _{2.5}	6.6	0.53	32	this work
Urban	Beijing, China	Winter/2014	PM _{2.5}	14.7	0.40	56	(Fang et al., 2017)
Urban	Beijing, China	Winter/2011	PM _{4.3}	15	0.50	55	(Zhang et al., 2014c)
Urban	Beijing, China	Winter/2013	PM _{2.5}	9.3	0.31	54	(Yan et al., 2017)
Urban	Guangzhou, China	Winter/2012/ 2013	PM _{2.5}	4.1	0.38	33	(Liu et al., 2014)
Urban	Guangzhou, China	Winter/2011	PM ₁₀	4.5	0.43	28.5	(Zhang et al., 2014c)
Urban	Xi'an, China	Autumn/2009	PM _{2.5}	5.1	0.28	31	(Pavuluri et al., 2013)
Urban	Xi'an, China	Autumn/2010	TSP	8.1	0.28	29	(Pavuluri et al., 2013)
Urban	Wuhan, China	Winter/2013	PM _{2.5}	13.7	0.45	37	(Liu et al., 2016)
Urban	Sapporo, Japan	Summer/Autum n/2010	PM ₃	1	0.43	15	(Pavuluri et al., 2013)
Urban	Sapporo, Japan	Summer/2011	TSP	1.1	0.24	12	(Pavuluri et al., 2013)
Urban	Sapporo, Japan	Spring/2010	TSP	1.1	0.31	11	(Pavuluri et al., 2013)
Urban	Sapporo, Japan	Autumn/2011	TSP	1.8	0.48	18.3	(Pavuluri et al., 2013)
Urban	Sapporo, Japan	Winter/2010	TSP	0.9	0.45	40.2	(Pavuluri et al., 2013)
Background	Jeju Island, Korea	Winter/2014	PM _{2.5}	2.2	0.66	50	(Fang et al., 2017)
Background	Jeju Island, Korea	Spring/2011	PM _{2.5}	2.0		37.5	(Kirillova et al., 2014a)
Background	Jeju Island, Korea	Spring/2011	TSP	3.0		25	(Kirillova et al., 2014a)
Average						33±14	
South Asia							
Background	Hainan, China	Annual 2005/2006	PM _{2.5}	3.9	0.54	18	(Zhang et al., 2014b)
Background	Hainan, China	Winter 2005/2006	PM _{2.5}	6.2	0.57	14.5	(Zhang et al., 2014b)
Background	Hainan, China	Summer 2005/2006	PM _{2.5}	1.4	0.40	17.7	(Zhang et al., 2014b)
Background	Hanimaadhoo, Maldives	Annual 2008/2009	TSP	0.5		17	(Kirillova et al., 2013)
Background	Sinhagad, India	Annual 2008/2009	TSP	3.0		24	(Kirillova et al., 2013)
Background	Hanimaadhoo, Maldives	Spring/2012	PM _{2.5}	0.6	0.62	14	(Bosch et al., 2014)
Urban	Delhi, India	Winter/2010/ 2011	PM _{2.5}	22.0		21	(Kirillova et al., 2014b)
Average						18±4	

Europe and USA							
Urban	Göteborg, Sweden	Winter/2005	PM _{2.5}	1.1	0.48	23	(Szidat et al., 2009)
Urban	Göteborg, Sweden	Summer/2006	PM _{2.5}	0.8	0.61	30	(Szidat et al., 2009)
Rural	Göteborg, Sweden	Winter/2005		1.2	0.53	27	(Szidat et al., 2009)
Rural/semi-urban	Stockholm, Sweden	Summer/2009	TSP			12	(Kirillova et al., 2010)
Urban	Zürich, Switzerland	Summer/2002	PM ₁₀	2.1	0.54	14	(Szidat et al., 2004)
Urban	Zürich, Switzerland	Winter/2008	PM ₁₀	2.8	0.60	26.8	(Zhang et al., 2013)
Urban	Moleno, Switzerland	Summer/2006	PM ₁₀	5.3	0.67	30	(Zhang et al., 2013)
Urban	Bern, Switzerland	Winter/2009	PM ₁₀		0.39	14	(Zhang et al., 2014c)
Urban	Atlanta, USA	Summer/2004	PM _{2.5}	2.3	0.59	26.5	(Weber et al., 2007)
Rural	Millbrook, USA	Annual/2006/2007	TSP		0.36	12	(Wozniak et al., 2012)
Rural	Harcum, USA	Annual/2006/2007	TSP		0.38	14	(Wozniak et al., 2012)
Regional background	Cesar, Netherlands	Annual/2011/2012	PM _{2.5}	2.3	0.65	21	(Dusek et al., 2017)
Average						21±8	

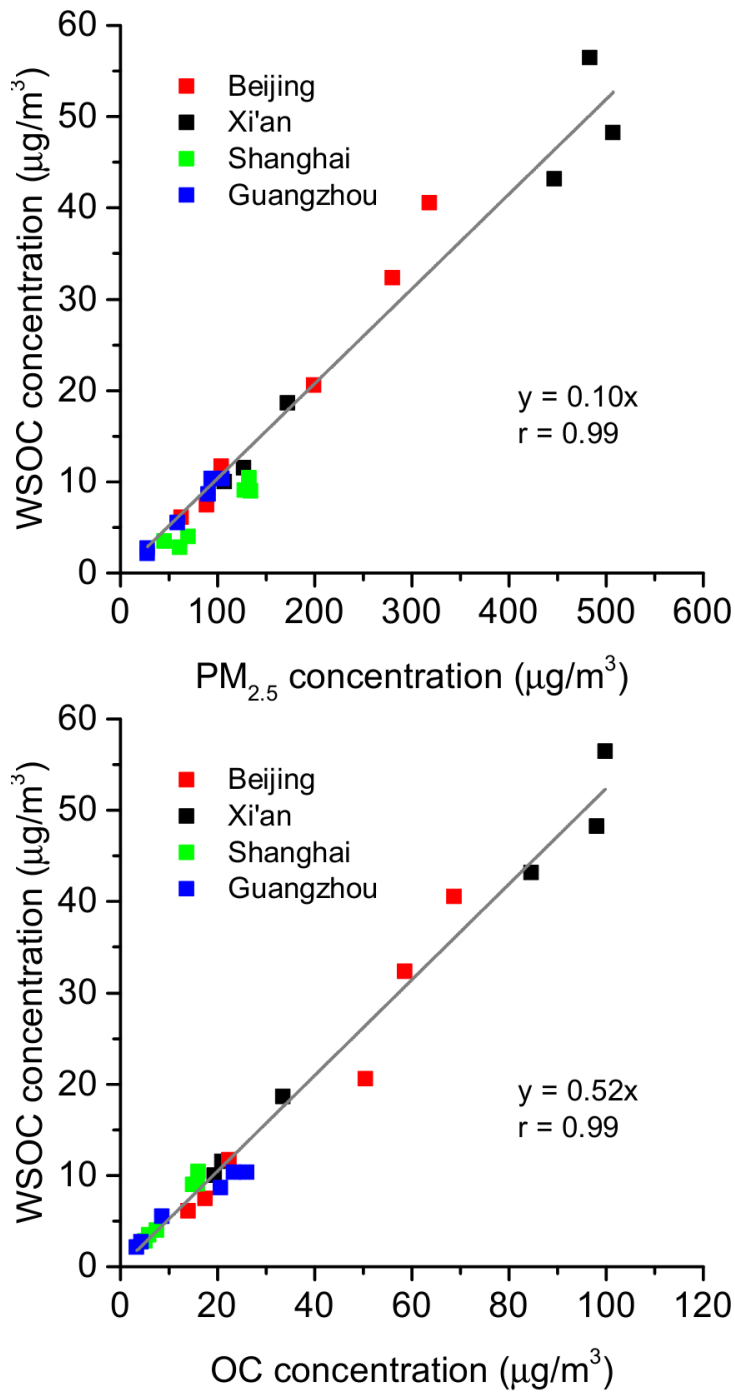


640

641 **Figure 1.** The AMS²-based source apportionment scheme of WSOC aerosols in this study.

642 See the main text for the equations (i.e., Eq. 4, 5, 9, 10 in the Sec. 2.5) and the offline-AMS &

643 PMF (see the Sec. 2.3).

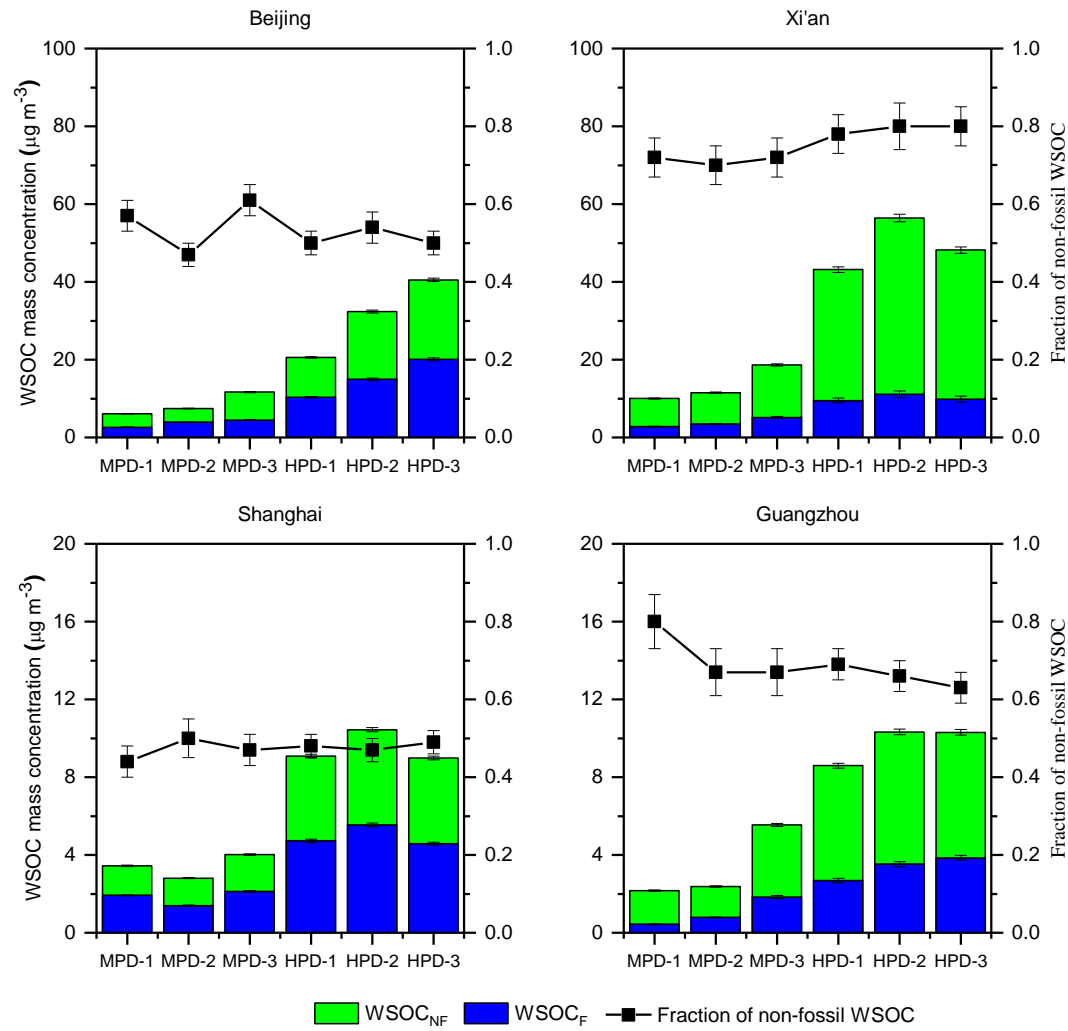


644

645 **Figure 2.** Linear relationships ($p < 0.01$) of WSOC with PM_{2.5} (top) and OC concentrations

646 (bottom).

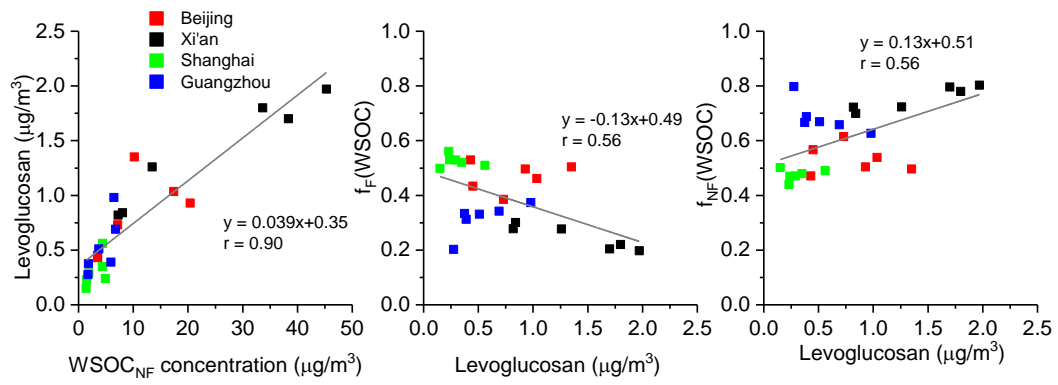
647



648

649 **Figure 3.** Mass concentrations ($\mu\text{g}/\text{m}^3$) of WSOC from non-fossil and fossil-fuel sources
 650 (WSOC_{NF} and WSOC_F , respectively) as well as non-fossil fractions of the WSOC aerosols from
 651 Beijing, Xi'an, Shanghai and Guangzhou during moderately polluted days (MPD) and heavily
 652 polluted days (HPD). Note the different scaling for different cities.

653

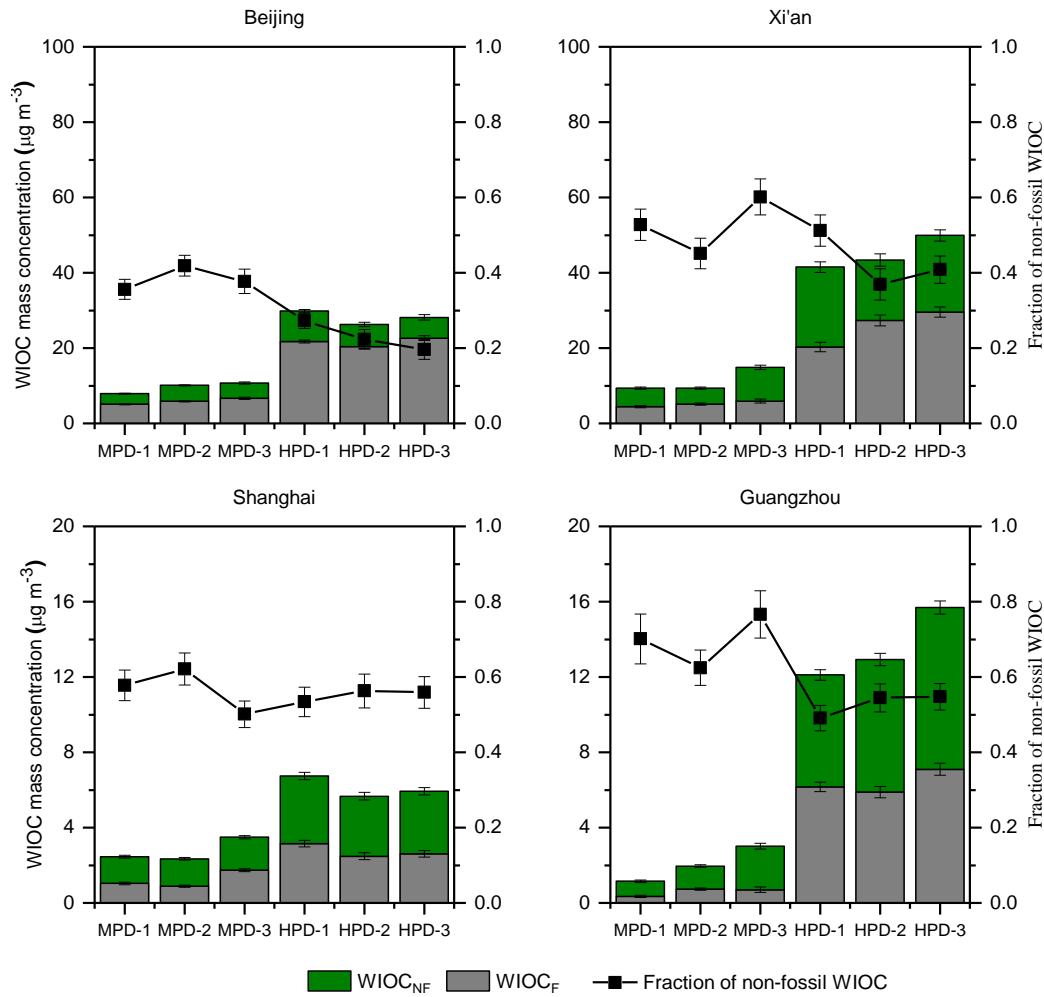


654

655 **Figure 4.** Relationships of non-fossil derived WSOC (WSOC_{NF}) and levoglucosan (left),

656 levoglucosan and fraction of fossil to WSOC ($f_{\text{F}}(\text{WSOC})$) (middle) and levoglucosan and

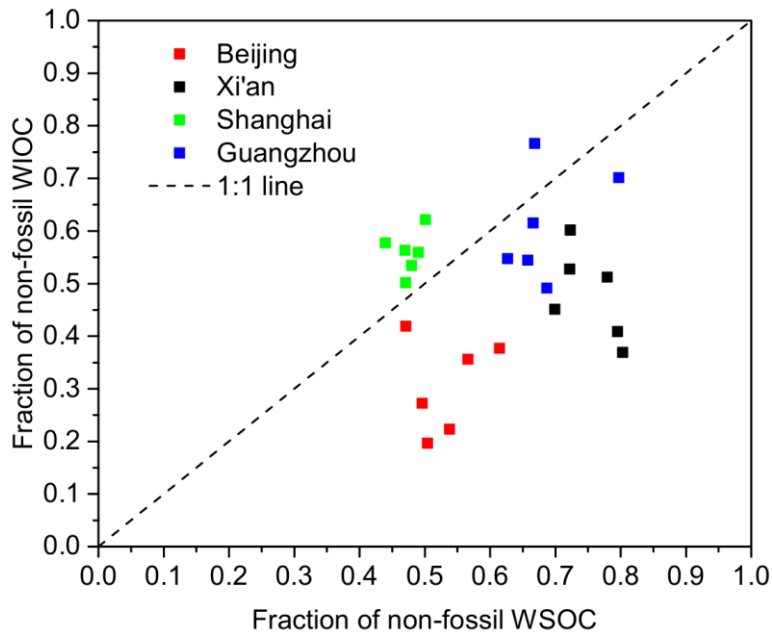
657 fraction of non-fossil to WSOC ($f_{\text{NF}}(\text{WSOC})$) (right).



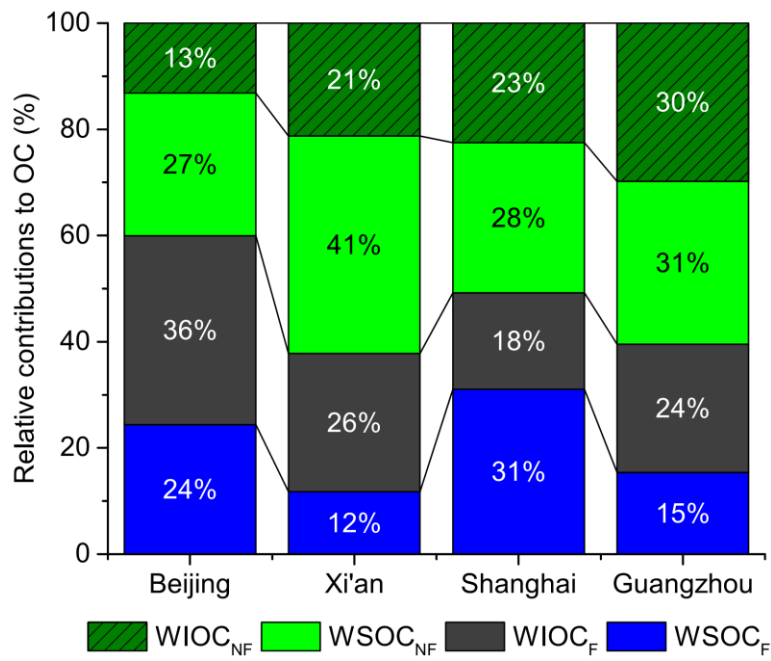
658

659 **Figure 5.** Mass concentrations ($\mu\text{g}/\text{m}^3$) of WIOC from non-fossil and fossil-fuel sources
 660 (WIOC_{NF} and WIOC_F, respectively) as well as non-fossil fractions in the WIOC aerosols from
 661 Beijing, Xi'an, Shanghai and Guangzhou during moderately polluted days (MPD) and heavily
 662 polluted days (HPD). Note the different scaling for different cities.

663



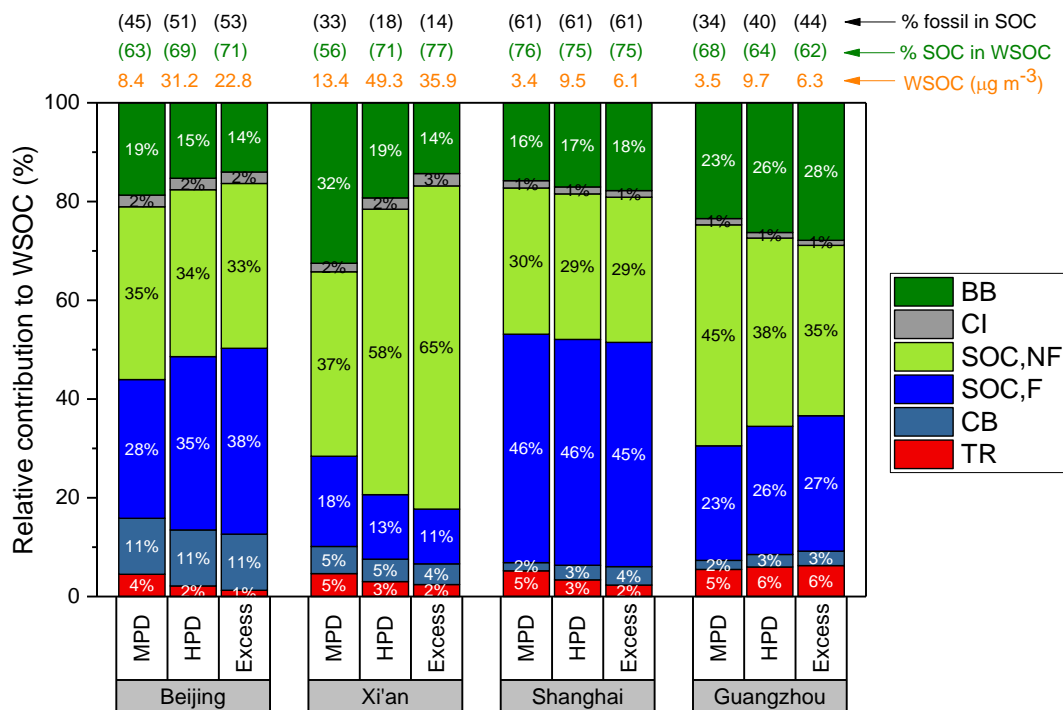
665 (a)



667 (b)

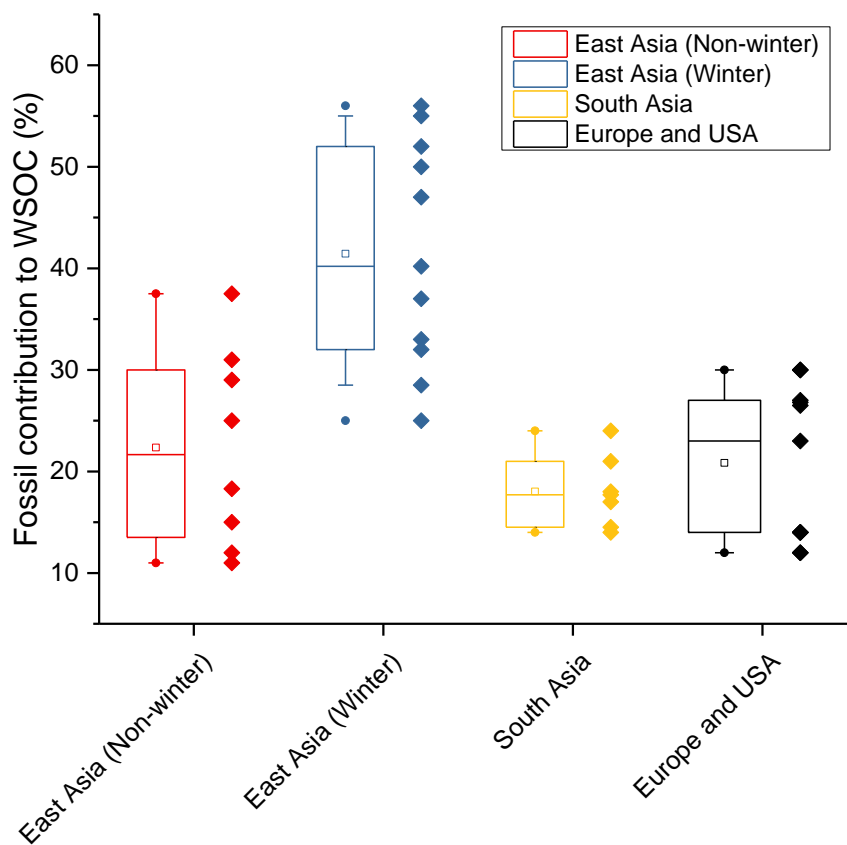
668 **Figure 6.** Relationship between the fraction of non-fossil WIOC and WSOC(a) and averaged
 669 relative contribution (%) to OC from WSOC and WIOC from non-fossil and fossil sources (b).

670



671

672 **Figure 7.** Relative contributions (%) to WSOC from biomass burning as well as secondary
 673 organic carbon (SOC) from fossil and non-fossil sources (WSOC_{SOC,F} and WSOC_{SOC,NF},
 674 respectively) in different cities during moderately polluted days (MPD) and heavily polluted
 675 days (HPD) as well as their corresponding excess (Excess=HPD-MPD). The numbers above
 676 the bars refer to the average WSOC concentrations and the SOC fractions (%) of WSOC.



677

678 **Figure 8.** Box-plot of the fossil contribution (%) to the WSOC aerosols in East Asia, South
 679 Asia, USA and Europe. The box represents the 25th (lower line), 50th (middle line) and 75th (top
 680 line) percentiles; the empty square within the box represent the mean values; the end lines of
 681 the vertical bars represent the 10th (below the box) and 90th (above the box) percentiles; the
 682 solid dots represents the maximum and minimum values; the solid diamonds represent the
 683 individual data (Table 1). The data from East Asia is grouped by the winter and non-winter
 684 seasons.